https://dx.doi.org/10.1016/j.jcsr.2023.108118

Experimental investigation on bolted inter-module connections and subassemblies of steel modular frames

Xiao-Zhou Han[1], Chen Wang[1,*], Xiao-Huang-Can He[2], Yi-Fei Hu[1,3], Tak-Ming Chan[1,3], Kwok-Fai Chung[1,3]

[1]Dept. of Civil and Environmental Engineering, The Hong Kong Polytechnic Univ., Hung Hom, Hong Kong, China.

[2]College of Civil Engineering, Guangxi University, Nanning, China

[3]Chinese National Engineering Research Centre for Steel Construction (Hong Kong Branch), The Hong Kong Polytechnic University, Hung Hom, Hong Kong, China

[*] Email: chen2.wang@polyu.edu.hk

Abstract

Modular construction, which involves prefabricating free-standing modules in a factory and assembling them on site to form a building, is gaining popularity worldwide. However, the existing inter-module connections generally require additional operation space and present difficulties in aligning adjacent modules quickly. Additionally, the global behavior of modular frames with inter-module connections under lateral loading is not well understood. To address these issues, this study investigates two types of inter-module connections (referred to as Type A and Type B), with high buildability and self-aligning features. Five pull-out tests were conducted to study the tensile behavior of the two types of inter-module connections, and five subassemblies of modular frames with these two types of inter-module connections were tested to study their global behavior under lateral loading. Based on the test results, the yielding distribution and development, strength, ductility, and failure modes were discussed for both types of inter-module connections under tensile loading and for the modular frames under lateral loading. Yielding of the steel plate (the end plate or anchoring plate), as anticipated, is found to be preferable to bolt failure for both types of inter-module connections to achieve greater ductility under tensile loading. Premature fracture of the beam-to-column weld was

identified as the main failure mode for all tested subassemblies of modular frames. As this early weld fracture prevented further development of both strength and deformation of the modular frame, it is recommended to avoid this failure mode in the design of modular frames.

Keywords: modular buildings; inter-module connection; steel modular frame; tensile behavior; failure modes

1 Introduction

Modular construction is an innovative building method where free-standing integrated modules, complete with finishes, fixtures, fittings, and other components, are manufactured off-site with controlled factory quality. These modules are then transported to the building site and assembled to form the entire building. Modular construction offers many benefits, including improved site safety, reduced on-site workload, better quality control, shorter construction periods, and less construction waste (Lawson et al., 2012 & 2014; Kamali & Hewage, 2016; Ferdous et al., 2019). In recent years, modular buildings have gained popularity in different parts of the world, including China, Singapore, Australia, and more (Navaratnam et al., 2019; Shan et al., 2019; Nadeem et al., 2021; He et al., 2021).

Inter-module connections are crucial components of modular structures as they not only affect the assembling speed of modular buildings but also significantly impact the overall response of the structure. Multiple studies at both the connection level and the system level have been conducted on steel modular frames in recent years. Chen et al. (2017a) proposed a novel connection design with an intermediate plug-in device and a beam-to-beam bolt system and conducted static and quasi-static cyclic tests on T-shaped connections. The results showed that gaps may occur between upper and lower columns which can affect the deformation patterns and bending demand distributions of the joint. Sanches et al. (2018) proposed an innovative vertical post-tensioned connection and carried out quasi-static cyclic tests to assess its seismic behavior. The results revealed that the proposed joint had similar lateral stiffness and strain distribution to the welded joint and a higher cumulative energy dissipation capability. An architecturally pleasing bolted connection with a welded cover plate was proposed by Deng et al. (2018). Tests under monotonic and cyclic load were performed and the results proved that all the specimens were able to develop full plastic strengths of the double beams under monotonic load. Lacey et al. (2019a) designed and fabricated a novel post-tensioned bolted

connection which showed satisfactory initial stiffness under shear and evaluated the impact of preloading and slip factor on the load-slip performance. Cho et al. (2019) proposed an effective steel frame modular system which adopted blind bolts and assessed the structural behavior of its beam-to-column joint. A novel bolted connection with tenon-gusset plate and long bolts through beams was put forward by Khan and Yan (2020). The finite element results indicated that bearing failure of the floor beam was caused by the gap formed between the upper and lower components of the joint. At the system level, modular frame tests and simulations to examine the seismic behavior of the modules assembled by pretension connections were carried out by Chen et al. (2017b). The connection presented comparatively rigid performance and the modular frame showed adequate resistance, stiffness and ductility within fortified intensity shake earthquake levels. Wang and Chan (2023) studied the response of steel modular frames through nonlinear response history analyses under a set of earthquake ground motions and found that the rotational stiffness of inter-module connections is critical to prevent soft-story mechanism of modular frames under strong earthquakes. He and Chan (2023) investigate the effect of stiffness properties of intra- and inter-module joints on the structural carrying capacity of braced steel modular structures and propose a joint classification system to facilitate design.

After reviewing existing research on inter-module connections, it was observed that a significant proportion of these connections require relatively large operating space and face difficulties in achieving quick alignment of modules (Lyu et al., 2021; Park et al., 2016; Lacey et al., 2019b; Nadeem et al., 2021). Additionally, the global behavior of modular frames under lateral loading is not well understood due to limited research, which has resulted in a notable redundancy in the existing structural systems of modular buildings (Navaratnam et al., 2019). To address these issues, two new types of bolted inter-module connections (referred to as Type A and Type B) were proposed in this study with the aim of achieving high buildability (i.e.,

simple and fast assembly, minimal operation space demand) and self-alignment. Firstly, the components and construction steps were elaborated for each of the two types of inter-module connections. Subsequently, five pull-out tests were conducted to study the tensile behavior of the proposed inter-module connections. Moreover, five subassemblies of modular frames with the proposed inter-module connections were tested to study the global behavior of modular frames under lateral loading. Based on the test results, the yielding distribution and development, strength, ductility, and failure modes were discussed for the two types of inter-module connections under tensile loading and the modular frames under lateral loading. Design recommendations were made for both inter-module connections and modular frames accordingly.

2 Proposed two types of inter-module connections

Following previous works reviewed in the Introduction, with the aim of improving buildability of inter-module connections, two new types of inter-module connections, referred to as Type A and Type B, are proposed and studied experimentally in this paper. The components, construction procedures, and features of the two connections are elaborated in this section.

2.1 Type A

As shown in Figure 1, the Type A inter-module connection consists of a shear key, a pre-welded steel endplate at the upper module corner, and a pre-welded steel endplate at the lower module corner. Openings will be made in endplates for locating the shear keys quickly. After the lower module is put in place, the shear key will be installed, which can in turn assist in locating the upper module and aligning the bolt holes in the connection. After the positioning of the upper module, bolts are fastened through the pre-welded endplates and the plate of the shear key to complete the assembly.

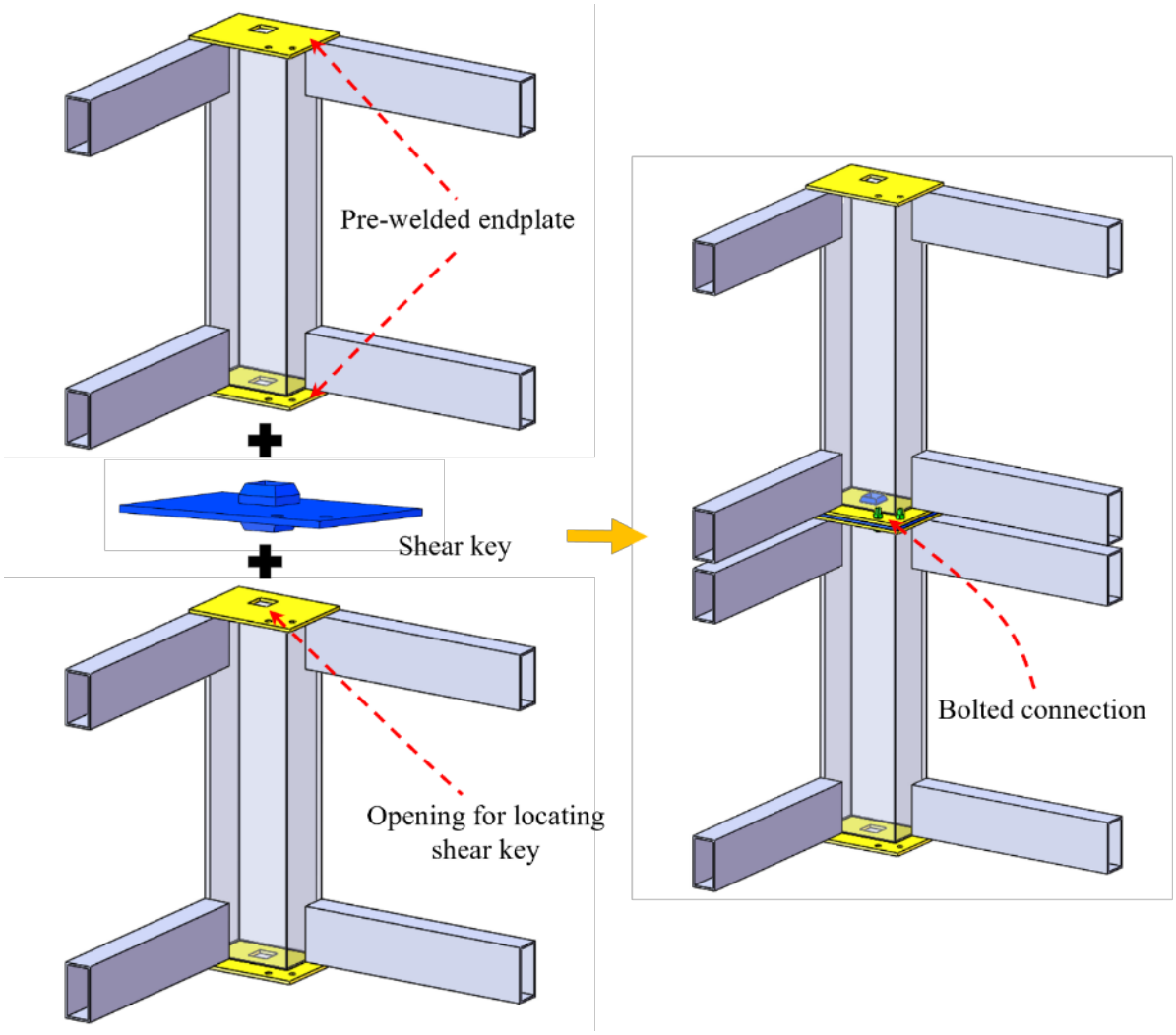

Figure 1. Illustration of Type A inter-module connection

The configuration of Type A connections is relatively simple, and the construction requires minimal onsite work without any onsite welding or wet trade work. With a shear key inserted into the columns of both the lower and upper module, Type A connections feature fast positioning of the upper module and self-aligning of the bolt holes. Additionally, Type A connections allow for vertical and horizontal connections between up to eight modules (i.e., joint of four lower and four upper modules). However, as the center of the columns is not aligned with the center of the bolt group, eccentric loading and even prying action will be exerted on the bolts when the connection is under tension, which is a disadvantage.

2.2 Type B

The components of Type B inter-module connections are illustrated in Figure 2. The shear key

components are made up of an end plate with the upper and lower tubes, and then the positioning plates are welded on the top and the bottom of tubes. The positioning plate features a central hole to enable a steel bolt to pass through it. Within each steel column of hollow section, two anchoring plates are shop welded with a central hole to allow a steel bolt to pass through. A nut is pre-welded on the bottom surface of the upper anchoring plate. An access opening is also provided at the bottom of the column of the upper module for installing the steel bolt.

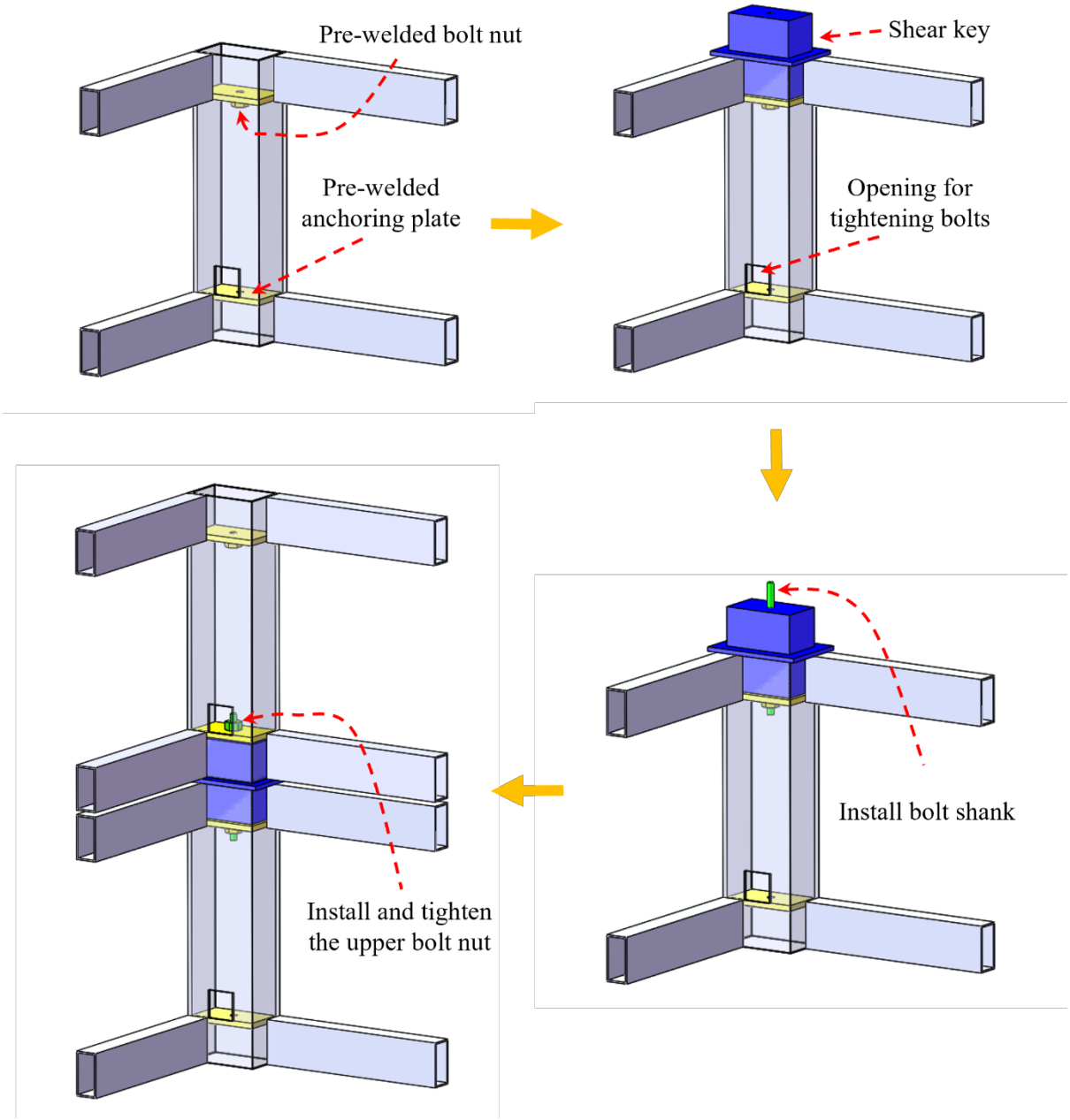

Figure 2. Illustration of Type B inter-module connection

In terms of the site assembly of Type B inter-module connections, after placing the lower module, the shear key component is inserted into the lower module column. Next, a vertical steel bolt will be installed through the positioning plate, anchoring plate, and pre-welded nut. Then, the upper module is lifted and placed on top of the lower module, with the shear key and the steel bolt serving as locating devices to facilitate fast and accurate positioning of the upper module and self-aligning of the bolt holes. Finally, a nut will be installed above the anchoring plate in the upper module through the column opening, and the bolt will be preloaded.

Type B inter-module connections require minimal onsite work, mainly bolt installation without any onsite welding or wet trade work. One worker can handle the installation, as verified by the following experiments. The shear key allows for fast and accurate positioning of the upper module and self-aligning of the bolt holes. The preloaded bolt lies in the middle of the columns and can provide direct axial connection between two columns. Similar to Type A connections, Type B connections can be used to provide both vertical and horizontal connections between up to eight modules (i.e., joint of four lower and four upper modules). Type B inter-module connections have been granted an HK patent (Hu et al., 2021) and a Chinese utility patent (Hu et al., 2022).

3 Experimental tests on inter-module connections

Inter-module connections play a crucial role in transferring forces between the upper and lower modules, especially when the modular structure is under lateral loading such as wind or earthquake. Specifically, inter-module connections will be subjected to significant shear and axial loading. For both Type A and Type B inter-module connections, the shear key is expected to take the majority of the shear force, which has been studied by previous studies (Lacey et al., 2019a). However, under axial loading, especially tensile loading, the load transfer mechanisms are unique for Type A and Type B inter-module connections. To characterize the behavior of the two types of inter-module connections under tensile loading, five full-scale

153 experimental tests (two Type A connections and three Type B connections) with various key
154 design parameters were conducted. Repetitive specimens, namely, CON-B-12 and CON-B-
155 12R, were deliberately included in the study to examine the potential influence of material and
156 geometry variations on the behavior of the inter-module connections.

157 **3.1 Test specimens and material properties**

158 In both Type A and Type B inter-module connections, the tensile force is transferred through
159 tension of bolts and out-of-plane loading of the connected steel plates. As such, the key design
160 parameters include the bolt diameter and the thickness of connected steel plates. To examine
161 the effect of these parameters, five specimens were designed, including two Type A
162 connections and three Type B connections, with different bolt diameters and thicknesses of the
163 steel plate. Figure 3 illustrates the dimensions, while Table 1 summarizes the detailed
164 information of the specimens. Prior to testing, geometric information was measured to verify
165 the accuracy of fabrication, and the results indicated acceptable fabrication quality.

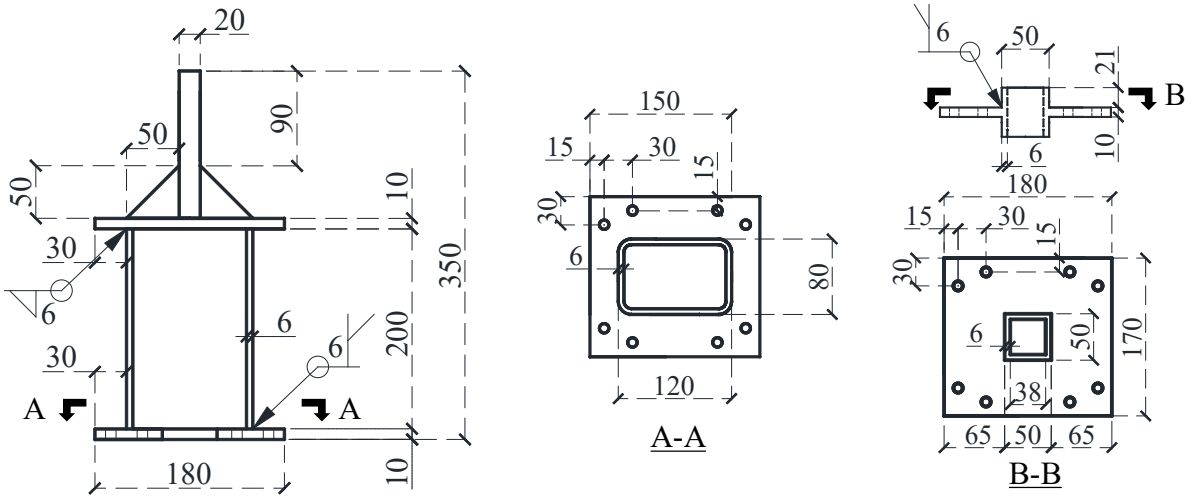

Type A Shear key

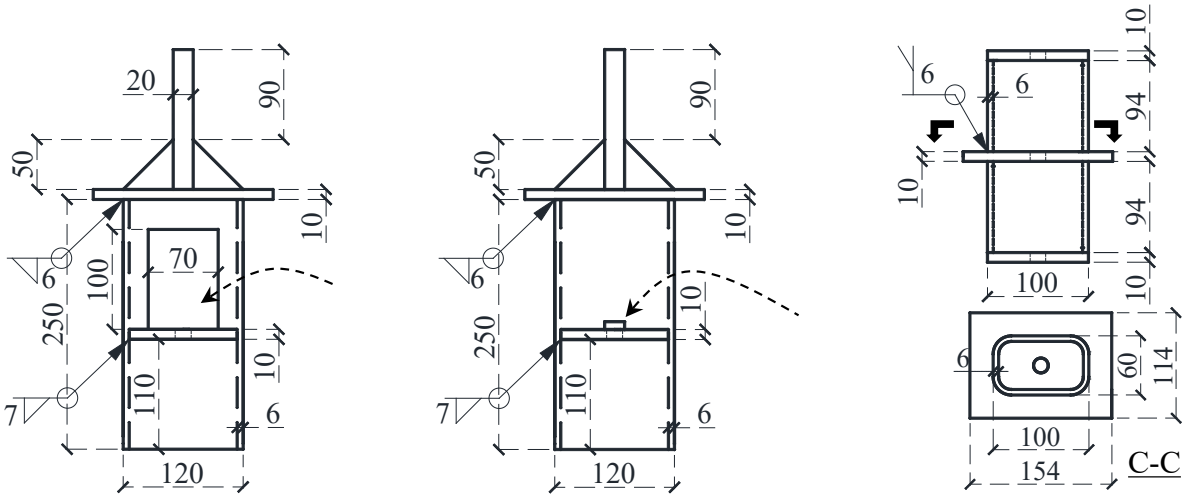

ype B Shear key

166

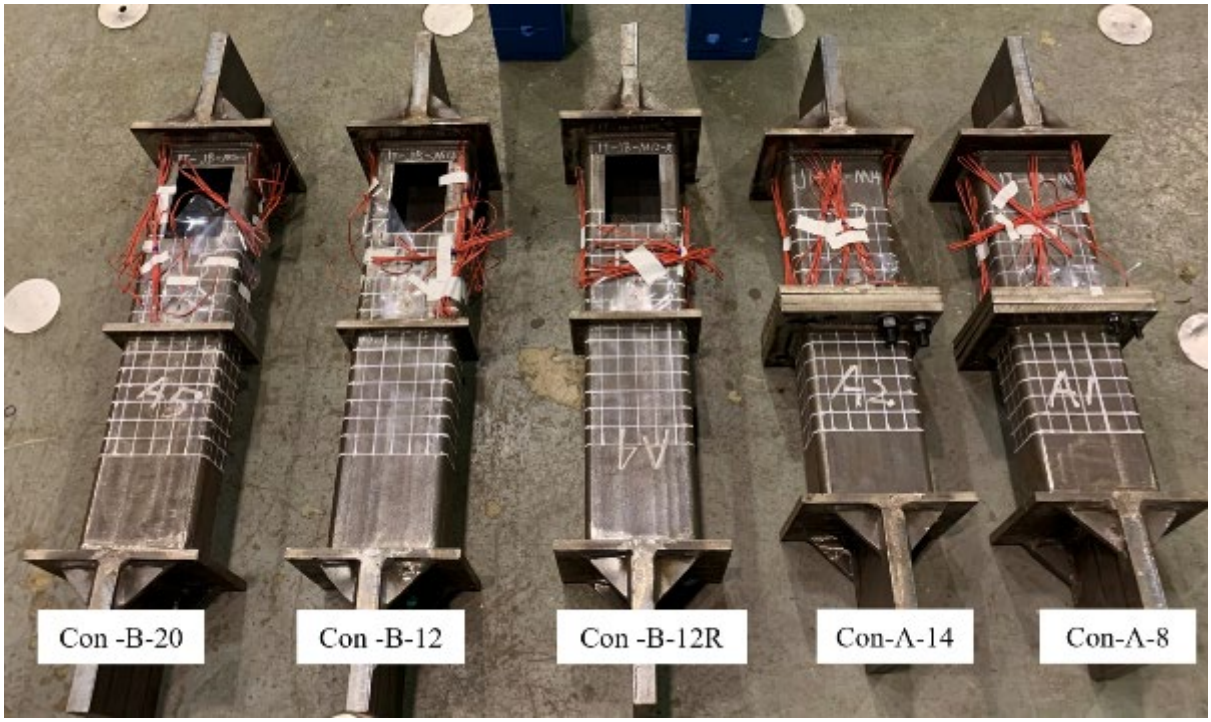

Figure 3. Dimensions of specimens of inter-module connections

Table 1. Test specimens of inter-module connections

Specimen ID	Type	Steel grade of endplate/ anchoring plate	Bolt grade	Bolt diameter (mm)	Endplate/anchoring plate thickness (mm)
Con-A-8	Type A	Q460	8.8	8	10
Con-A-14	Type A	Q460	8.8	14	10
Con -B-12	Type B	Q460	6.8	12	10
Con -B-12R	Type B	Q460	6.8	12	10
Con -B-20	Type B	Q235	8.8	20	6

To obtain the actual material properties of the test specimens, tension coupon tests were conducted for each component including bolts following the standard EN ISO 6892-1:2019. Considering notable differences in material properties between the flat and the corner regions of steel hollow sections, tensile coupons were extracted from both the flat region and the corners for each steel hollow section. The tensile coupon test results are summarized in Table 2.

178 **Table 2.** Measured material properties of test specimens

Component	Component Applied	Flat Coupons					Corner/Circular Coupons				
		E	$f_{y,f}$	$f_{u,f}$	$\varepsilon_{u,f}$	$\varepsilon_{f,f}$	E	$f_{y,c}$	$f_{u,c}$	$\varepsilon_{u,c}$	$\varepsilon_{f,c}$
		GPa	MPa	MPa	%	%	GPa	MPa	MPa	%	%
120 × 80 × 6 S460 Tube	Beams and columns of all specimens	177	488	569	8.36	21.47	121	604	676	1.94	2.26
		186	480	569	8.73	23.44	202	603	662	2.03	4.66
		195	456	570	5.61	7.76	-	-	-	-	-
		179	480	543	3.93	5.80	-	-	-	-	-
100 × 60 × 6 Tube	Joint B Shear Keys	202	516	582	5.83	23.65	131	596	644	2.26	11.08
		202	528	585	6.89	25.56	144	649	696	1.62	2.06
50 × 50 × 6 Tube	Joint A Shear Keys	218	581	666	1.09	2.24	211	544	646	1.39	4.99
		196	625	657	0.82	0.87	135	641	686	2.05	12.02
6 mm thick Plate	Anchoring Plates	211	242	377	23.72	38.00	-	-	-	-	-
		205	247	376	23.11	37.81	-	-	-	-	-
		204	245	377	23.02	39.22	-	-	-	-	-
10 mm thick Plate	Anchoring, Positioning and End Plates	204	428	534	18.26	37.13	-	-	-	-	-
		204	422	531	17.38	36.97	-	-	-	-	-
		207	415	530	17.72	36.65	-	-	-	-	-
M12 Grade 6.8 Bolt	Joint B Assembly	-	-	-	-	-	223	502	585	5.01	14.18
M20 Grade 8.8 Bolt	Joint B Assembly	-	-	-	-	-	205	710	797	5.66	12.88

179

180 **3.2 Test setup and instrumentation**

181 The test setup and instrumentation for all inter-module connection specimens are presented in
182 Figure 4. The two ends of the specimen were tightened by the grips of an in-house 500 kN
183 INSTRON multi-functional tension/compression testing machine. Monotonic tensile loading
184 was applied until failure of the specimens. Four displacement transducers (LVDT 1-4) were
185 utilized to measure the axial elongation of each specimen under tensile loading. Additionally,
186 strain gauges were mounted on the column (SG1-4) and the endplate (SG5-7) to monitor the
187 strain development.

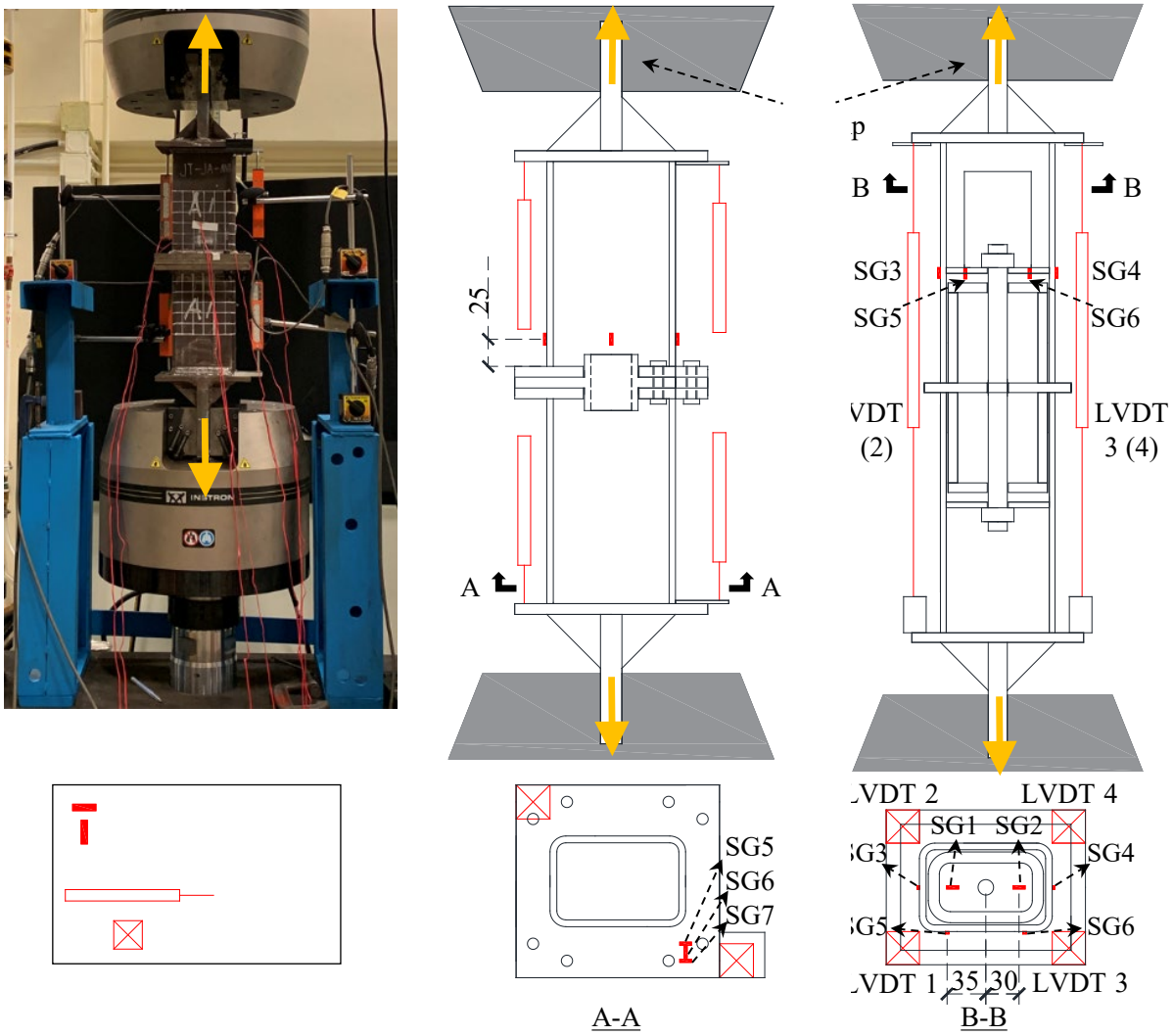

Figure 4. Test setup and instrumentation for inter-module connections (Unit: mm)

4 Experimental tests on subassemblies of modular frames

4.1 Test specimens and material properties

To study the behavior of modular frames utilizing the proposed inter-module connections under lateral loading, five experimental tests were conducted on subassemblies of modular frames. Each subassembly consists of components of the upper module (i.e., a column and a floor beam), components of the lower module (i.e., a column and a ceiling beam), and an inter-module connection, as shown in Figure 5. Among the five subassemblies, welding was used in the inter-module connection of one specimen, i.e., specimen SA-W, which served as the reference specimen, while Type A inter-module connection was adopted in one specimen and

200 Type B inter-module connection was adopted in three specimens. The study intentionally
201 included repetitive specimens, specifically SA-B-20 and SA-B-20R, to investigate the potential
202 impact of material and geometry variations on the behavior of the modular frame. The
203 information of the five specimens is listed in Table 3. The same beam/column sections were
204 used for all the five specimens, whose dimensions are shown in Figure 5. Tensile coupon tests
205 were conducted for each component of the subassemblies to obtain the actual material
206 properties of the test specimens, whose results are listed in Table 2. It is noted that as the same
207 batch of steel plates and sections were used for both the inter-module connections and
208 subassemblies of modular frames, tensile coupon tests were conducted based on the component
209 types rather than the specimens.

210 **Table 3.** Information of test subassemblies of modular frames

Specimen	Inter-module connection type	Steel grade of endplate/ anchoring plate	Bolt grade	Bolt diameter (mm)	Endplate/ anchoring plate thickness (mm)
SA-W	Welded	Q460	-	-	-
SA-A-8	Type A	Q460	8.8	8	10
SA-B-12	Type B	Q460	6.8	12	10
SA-B -20	Type B	Q460	8.8	20	10
SA-B -20R	Type B	Q460	8.8	20	10

211

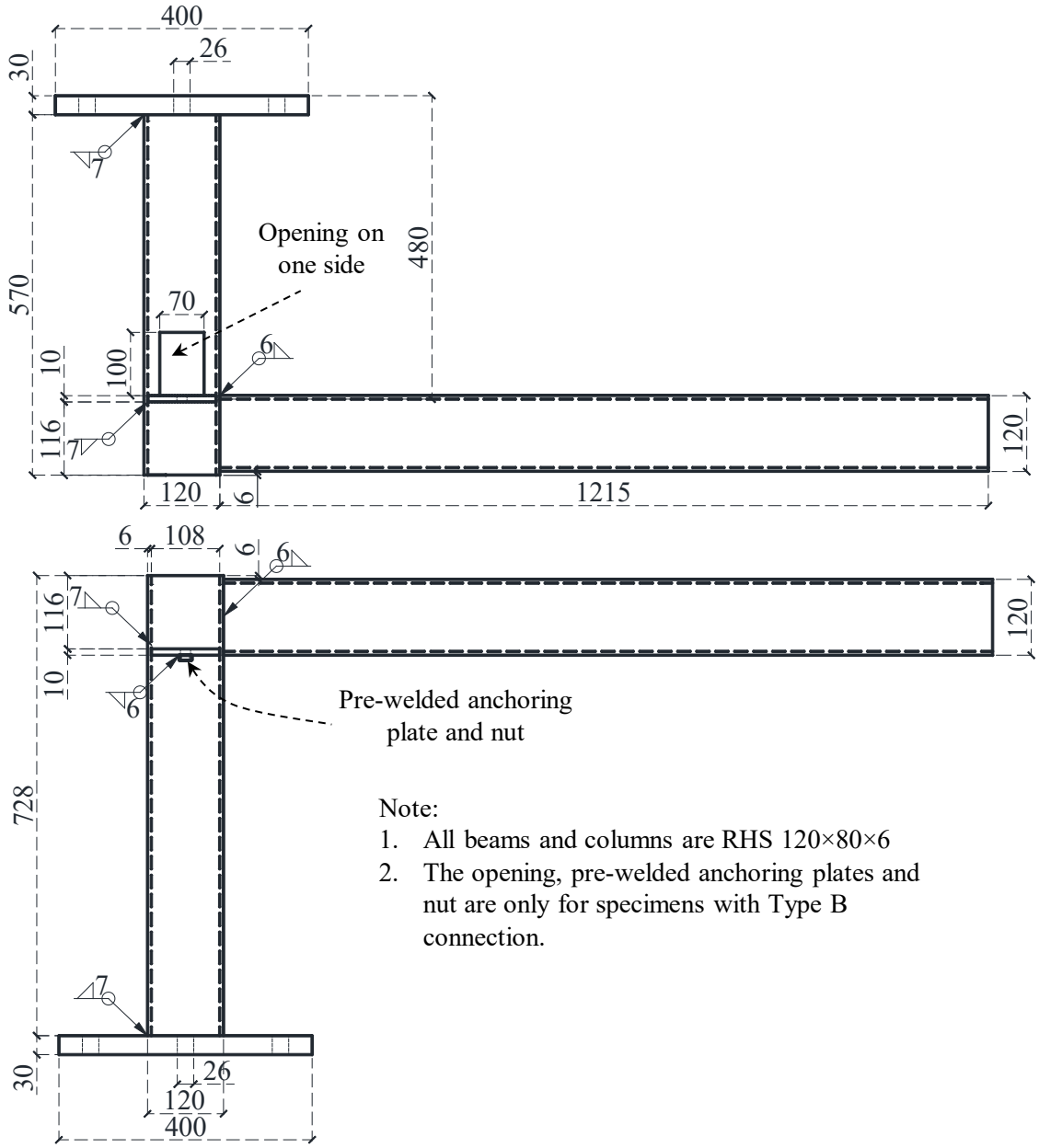

212

213 **Figure 5.** Dimensions of subassemblies of modular frames (Unit: mm)

214 **4.2 Test setup and instrumentation**

215 Figure 6 shows the test setup and instrumentation for all the test subassemblies of modular
216 frames. Steel plates with a thickness of 30 mm were welded to columns at their upper and lower
217 ends, and they were connected to the loading frame to restrain both the translational and
218 rotational movement of column ends. At the beam end, a binding device was installed to
219 restrain the ends of the floor beam and the ceiling beam and to ensure they have the same
220 rotational and vertical movement in the frame plane. Steel rods with smooth surfaces were

placed between the floor beam and ceiling beam at the end to enable the relative horizontal movement between the two beams. The binding device was connected with a hydraulic jack through a pin. Vertical load was applied by a hydraulic jack and increased until failure of the specimens.

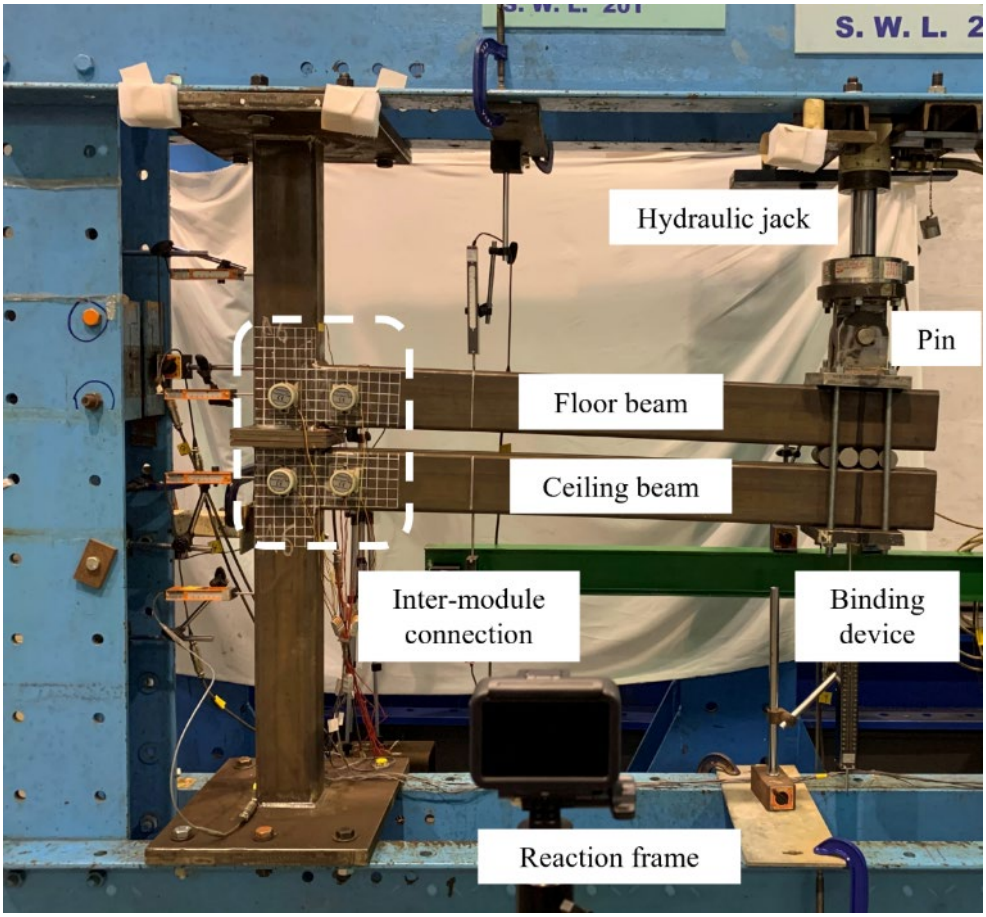

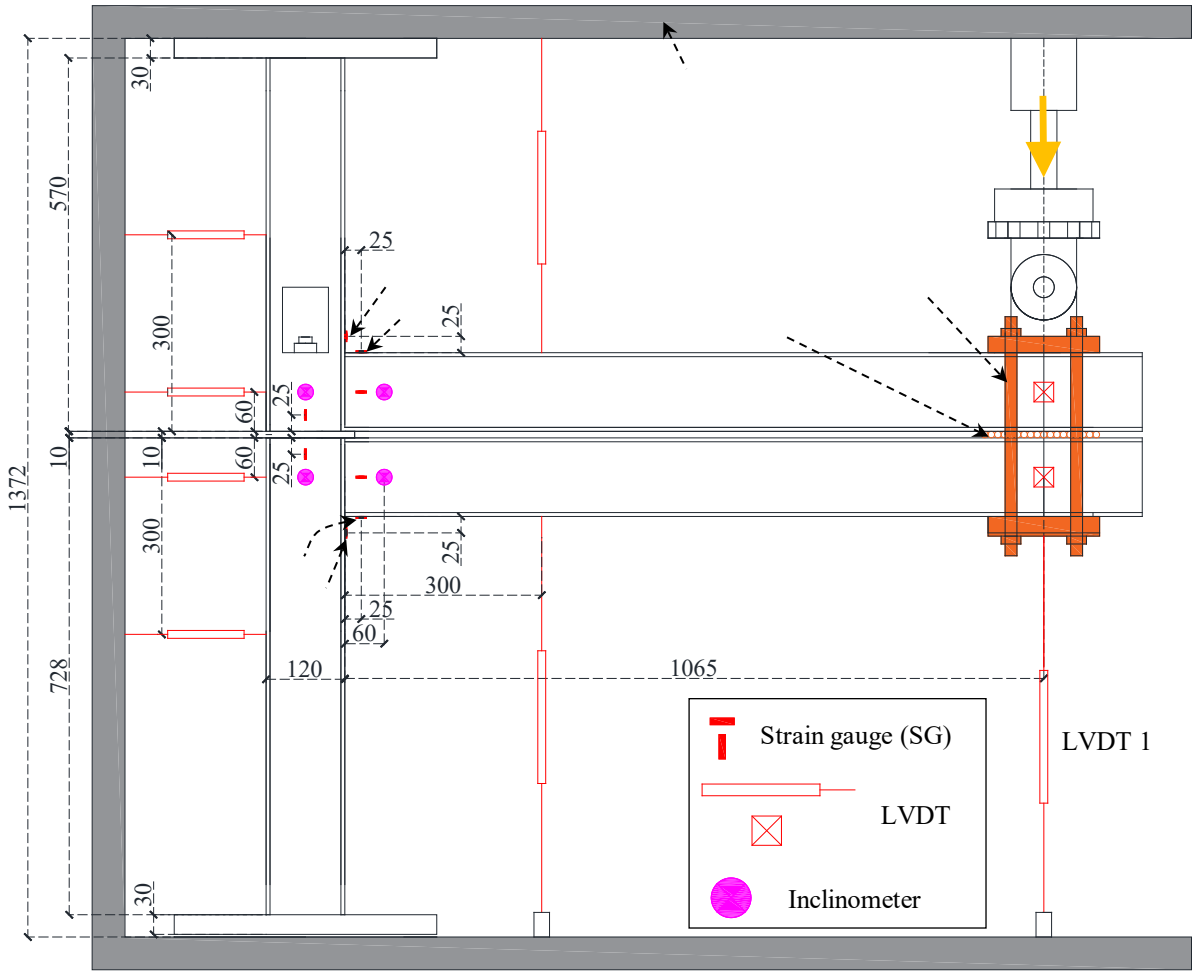

Figure 6. Test setup and instrumentation for subassemblies of modular frames (Unit: mm)

A total of nine displacement transducers were employed to measure the displacements at specified locations for each test. The vertical displacement of the loading point was recorded by LVDT 1. LVDTs 2 and 3 monitored the vertical displacement of beams to determine the elastic deformation of the beams by comparing their data to that from LVDT 1. The column rotation was measured by the LVDT 4 to LVDT 7 installed on the left side of the column. In addition, LVDTs 8 and 9 located at beam end were positioned perpendicularly to the loading direction to measure the out-of-plane displacement of the beams. Four inclinometers (I-1 to I-4) were used to measure the rotation angles near the inter-module connection. Strain gauges were mounted on column ends, beam ends, bolts and other specified locations to monitor the strain development at different locations.

Such boundary and loading conditions were similar to the loading condition of the T-shaped subassembly in the full modular frame. Moreover, the T-shaped subassembly includes key components that contribute to the load path within the modular frame, such as the upper story's column and floor beam, the lower story's column and ceiling beam, and the inter-module connection. As such, testing the T-shaped subassemblies, with the adopted test setup in this study, can provide insights into the behavior of modular frames under lateral loading.

5 Test results and discussion

5.1 Response of inter-module connections

In this section, the experimental observations and test results for the inter-module connections are presented and discussed. The deformed shapes and failure modes for each specimen are presented in Figure 7. The extension of the inter-module connections between the upper and the lower endplates can be determined based on the data collected by LVDTs. The load-extension curves for the five specimens are presented in Figure 8.

During the test on specimen CON-A-8, separation was observed on the opposite side of the bolts with the increase of loading as shown in Figure 7(a). Notable deformations in the bolts were observed, and failure of the bolts was expected to occur soon. For the concern of safety, the loading was halted at a load level close to the predicted tensile resistance of the two bolts. For specimen CON-A-14, the column end plates experienced significant bending deformation, which led to gaps between the three steel plates fastened by the bolts, as shown in Figure 7(b). As the load further increased, the gap size increased, and one of the bolts fractured at an ultimate load of 150 kN.

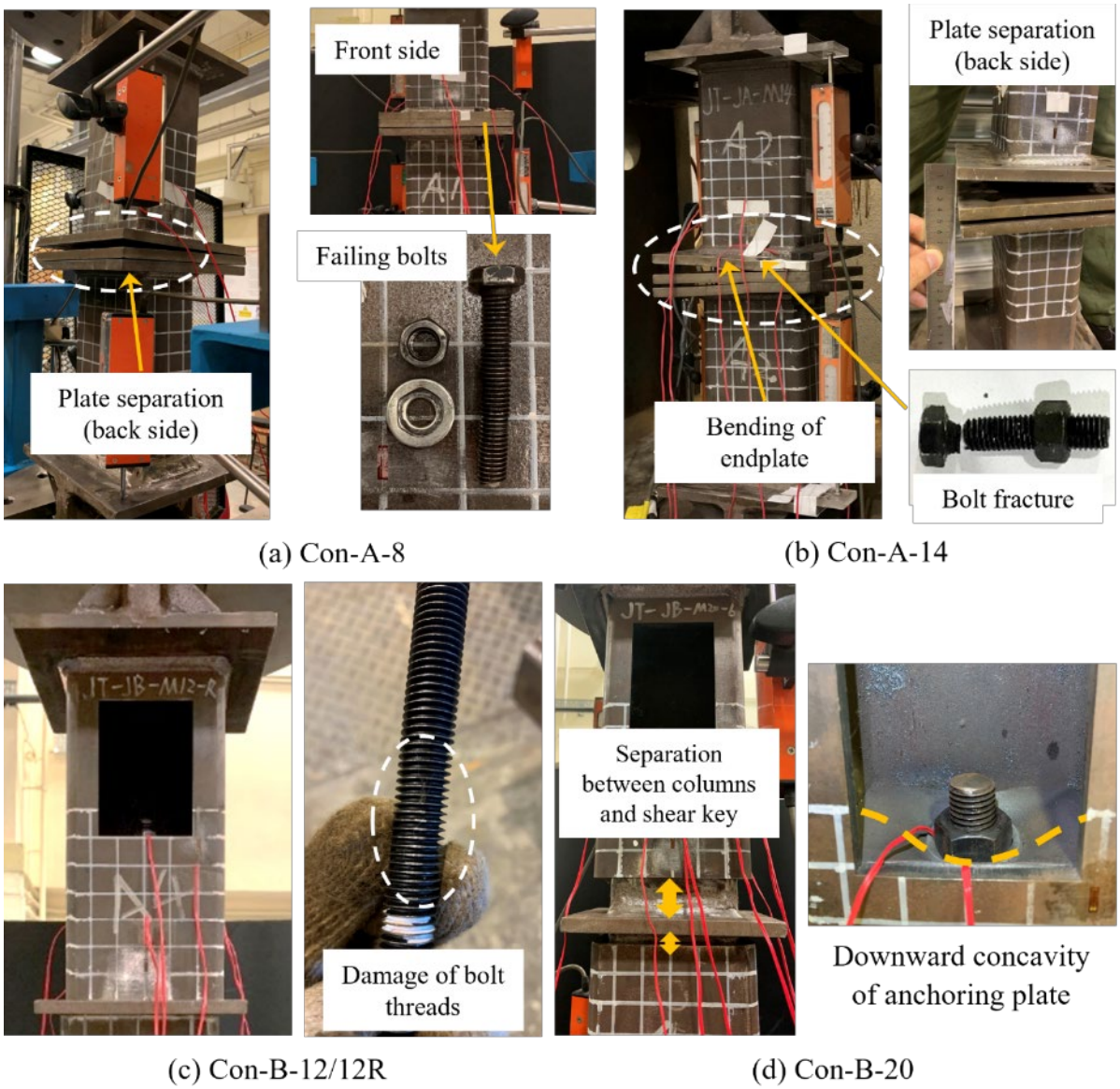

Figure 7. Deformed shapes and failure modes of inter-module connections under tension

Specimens CON-B-12 and CON-B-12R exhibited similar responses: no noticeable deformation was observed until failure of the bolt in the form of bolt thread damage as shown in Figure 7(c). Notably, the consistent results obtained from these repetitive specimens indicate that the structural response of the inter-module connections does not exhibit significant randomness. This observation strengthens the reliability and validity of the obtained test results. For specimen CON-B-20, the bolt remained intact throughout the test, while significant concavity deformation was observed in the anchoring plate as shown in Figure 7(d). As can be seen in the load-extension curve of specimen CON-B-20, after the initial linear elastic phase,

the stiffness of the specimen gradually decreased to almost zero at an extension of around 12 mm, after which the specimen regained part of the stiffness. The regaining of stiffness is believed to be caused by the formation of the membrane action of the anchoring plate after large out-of-plane deformation. Specimen CON-B-20 exhibited a much larger extension at the maximum load than specimens CON-B-12/12R, i.e., 34 mm versus 1.2 mm, which implies a preference for the out-of-plane deformation of anchoring plates to the bolt failure in order to achieve ductile behavior of Type B inter-module connections under tensile loading.

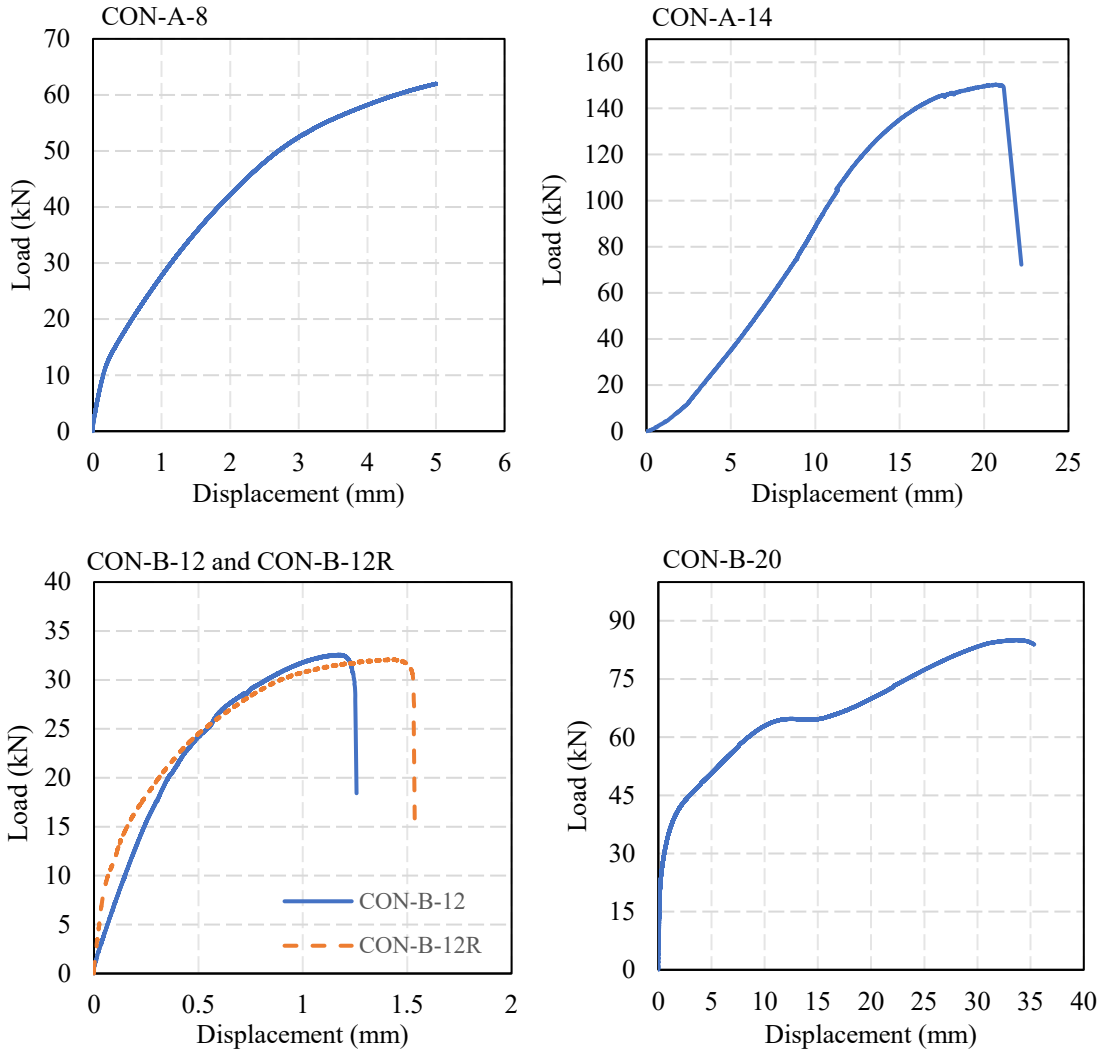

Figure 8. Applied load-displacement curves of inter-module connections

However, as the connections were not loaded in a cyclic manner, the cyclic behavior and the damping capacity of the connections could not be characterized. As many lateral loads, such

281 as earthquake excitation, are cyclic in nature, it is essential to investigate the cyclic behavior
282 and damping capacity of the connections in further studies.

283 **5.2 Response of subassemblies of modular frames**

284 In this section, the experimental observations and test results for the subassemblies of modular
285 frames are presented and discussed. The deformed shapes and failure modes for each specimen
286 are presented in Figure 9. The relationships between the applied load by the hydraulic jack and
287 the vertical displacement of the binding device at the beam end are presented in Figure 10. For
288 the reference specimen SA-W with welded inter-module connection, weld fracture was firstly
289 observed at the interface between the column and the top flange of the ceiling beam, and
290 developed in a fast manner which resulted in an abrupt drop in the resistance, during which
291 fracture was also observed at the interface between the column and the top flange of the floor
292 beam, as shown in Figure 9(a). No noticeable deformation was observed in the inter-module
293 connection region. The load reached a maximum value of 118 kN at a vertical displacement of
294 42 mm.

295 For Specimen SA-A-8, separation occurred between the three bolted plates on the side away
296 from the bolts, with gaps increasing as loading increased, as shown in Figure 9(b). Noticeable
297 bending deformation was observed in the endplate of the upper module column. This indicated
298 that the inter-module connection was subjected to notable bending, and such bending was not
299 transferred effectively between the two modules through Type A inter-module connection. At
300 a vertical displacement of around 40 mm, weld fracture was firstly observed at the interface
301 between the column face and the top flange of the ceiling beam, and rapidly propagated
302 throughout the entire beam-to-column weld which resulted in an abrupt drop in the resistance.
303 Fracture was also observed at the interface between the column and the top flange of the floor
304 beam during this phase.

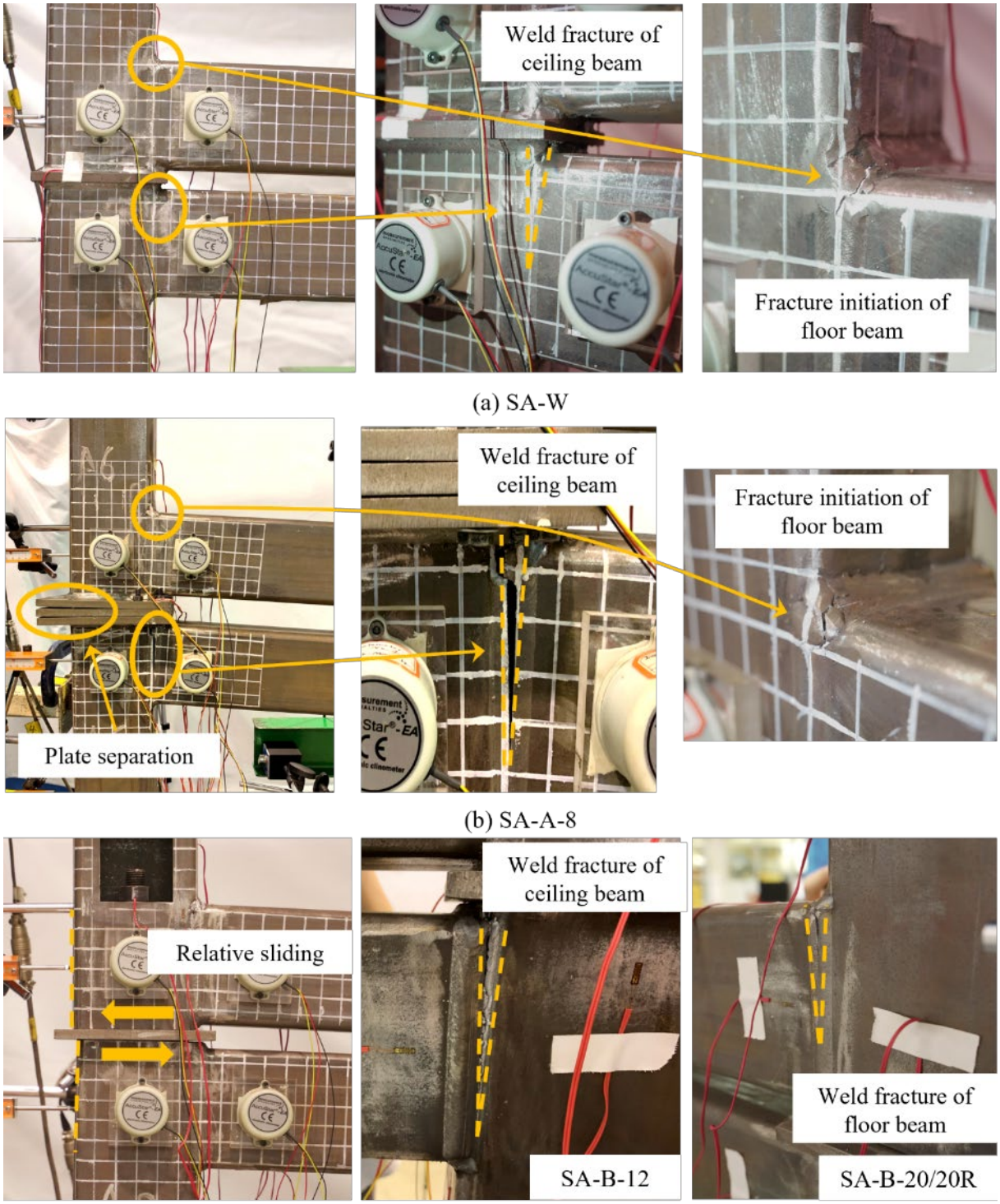

305

306 **Figure 9.** Deformed shapes and failure modes of subassemblies of modular frames

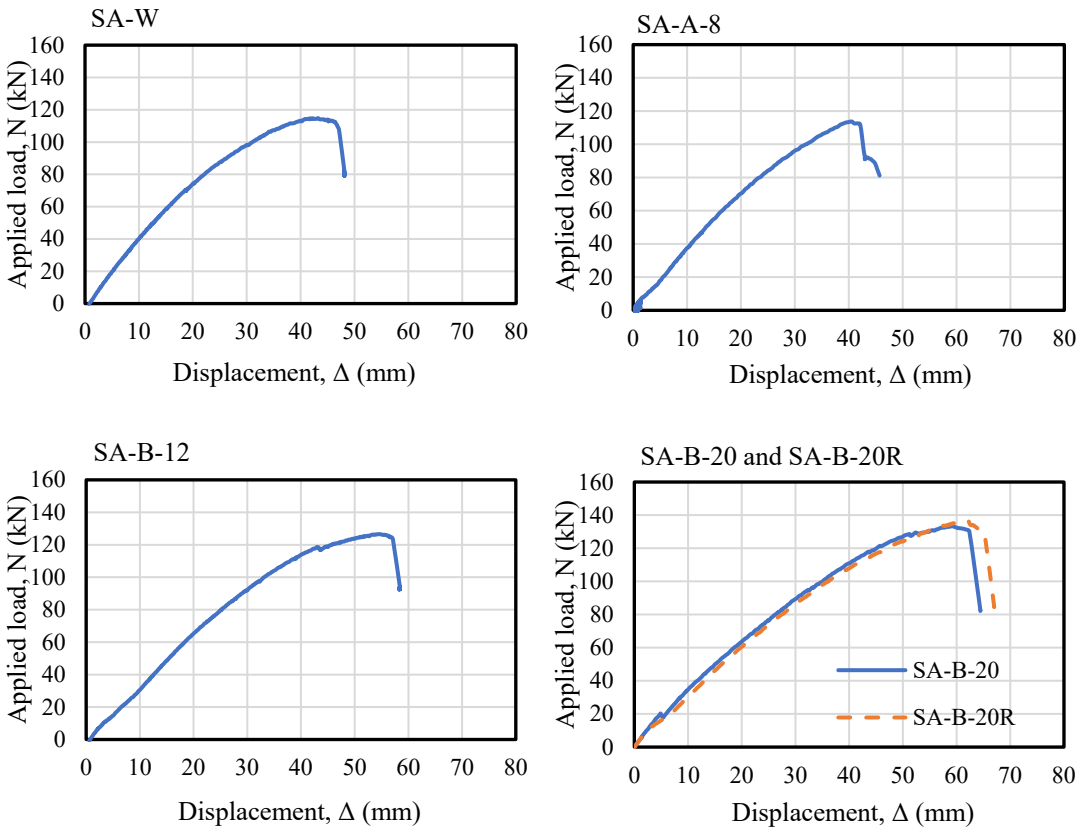

Figure 10. Applied load-displacement curves of subassemblies of modular frames

For specimens with Type B inter-module connections, similar experimental observations were obtained. During the initial loading phase, relative sliding between the upper and lower columns was observed in the inter-module connection, as shown in Figure 9(c). The magnitude of such sliding increased with the loading level and stopped increasing when it reached a value close to the difference between the inner dimension of the column and the outer dimension of the shear key. This was due to the presence of initial fabrication tolerance between the shear key and the columns. The relative rotation of the two beam-to-column panel zones resulted in the relative sliding in Type B inter-module connections. After the shear key contact with the columns, the relative sliding was restrained. Throughout the loading process, most of the deformations developed at the beam ends and the beam-to-column panel zone. The upper module column stayed in close contact with the lower module column. As the inter-module connections were subjected to bending as revealed by Specimen SA-A-8, the absence of

322 separation between the two columns suggested a better flexural bending continuity of Type B
323 inter-module connections than Type A. For all the specimens with Type B inter-module
324 connections, no deformation was observed near the opening which suggests that the position
325 of opening in the test specimens (i.e., above the beam-to-column panel zone) is reasonable.
326 However, it is worth noting that the openings were in the leg of the hollow sections that is
327 parallel to the plane of loading, and more research is needed to study the effect of the opening
328 in the case where the column is subjected to bi-axial bending. In the final phase, weld fracture
329 initiated and developed in a fast manner in the beam-to-column weld. However, the weld
330 fractures developed at different locations among the three specimens: the floor beam-to-column
331 interface for specimens SA-B-20 and SA-B-20R, and the ceiling beam-to-column interface for
332 specimens SA-B-12, as shown in Figure 9(c). Similarly, consistent results were obtained for
333 the repetitive specimens SA-B-20 and SA-B-20R, indicating the response of modular frames
334 is not subject to substantial randomness.
335 The maximum displacements of the three specimens with Type B inter-module connections,
336 were 57 mm, 63 mm and 63 mm. They are larger than those of the specimens with welded and
337 Type A inter-module connections (i.e., 47mm and 40 mm, respectively). As the bending
338 moments at the beam ends were similar, such large differences in maximum displacements
339 were believed to be related to the amount of welding at the inter-module connection region.
340 Specifically, for Type B inter-module connections, the only welding involved was the welding
341 connecting the beam and column. However, for Type A inter-module connections and the
342 welded inter-module connections, extra welding was required to connect the column with the
343 endplate, and these extra welds were very close to the beam-to-column welding. More welding
344 is expected to create a more sophisticated heat-affected zone and may introduce more welding
345 defects. This was also verified by the fact that, for both specimens with welded and Type A
346 inter-module connections, fractures initiated in the ceiling beam-to-column weld which was

close to the extra welds. In contrast, for specimens with Type B inter-module connections, fractures initiated either in the floor beam-to-column weld or the ceiling beam-to-column weld. It is worth noting that the experimental results consistently indicated that the failure mode of all tested T-shaped subassemblies was the fracture of beam-to-column welds. This failure mode can be attributed, in part, to initial defects present in the welds. Furthermore, the additional welds in the inter-module connections may contribute to the deterioration of the quality of the beam-to-column welds. Additionally, the critical bending moment at the beam-to-column welds played a significant role in the observed failure. These experimental results underscore the vulnerability of beam-to-column welds in modular frames when subjected to lateral loading. Consequently, it is imperative to strengthen and enhance the quality of these welds to prevent premature fracture and achieve a higher level of ductility for the entire modular frame.

5.3 Strain development in inter-module connections

The key findings based on the data collected from the strain gauges on inter-module connections will be discussed in this section. It is noted that the yield strain limit of a component is calculated as the ratio of the yield strength obtained through tension coupon tests to the steel elastic modulus, which are listed in Table 2. For specimens with Type A inter-module connections, the strain development in the four column faces was presented in Figure 11. Strain gauge SG1 was found to experience tensile strain while all the other three strain gauges experienced compression strains. The magnitude of SG1 was larger than those of the other three strain gauges. Those differences were resulted from the loading eccentricity in Type A inter-module connections. Under tensile loading, the force was transferred from the upper column through the bolts to the lower column. As the column face on which SG1 was attached is closer to the bolts, tensile strain was developed. In terms of the low strain level of SG3, it is believed to be caused by the fact that the location of SG3 was not in the main force-transferring path.

Figure 12 shows the strain development in all the monitored positions for specimen CON-A-14. Significant plasticity was developed between the two bolts which is consistent with the experimental observation of notable bending of the endplate along the line of the two bolts, while the column remained elastic. This result confirmed that one of the yield mechanisms of Type A inter-module connections under tensile loading is the plastic bending of the endplate along the line of the bolts.

For Type B inter-module connections, the bolt and anchoring plates play the key role in transferring tensile force between columns. Figure 13 presents the strain developments in the bolt and the anchoring plate of specimen CON-B-20. It confirms that the bolt in specimen CON-B-20 remained elastic while remarkable plasticity developed in the anchoring plate. Given the fact that specimen CON-B-20 exhibited the largest deformation capacity while specimens CON-B-12/12R which failed by bolt failure showed much smaller deformation capacities, it is recommended to design the bolt to be stronger than the anchoring plate for Type B inter-module connections.

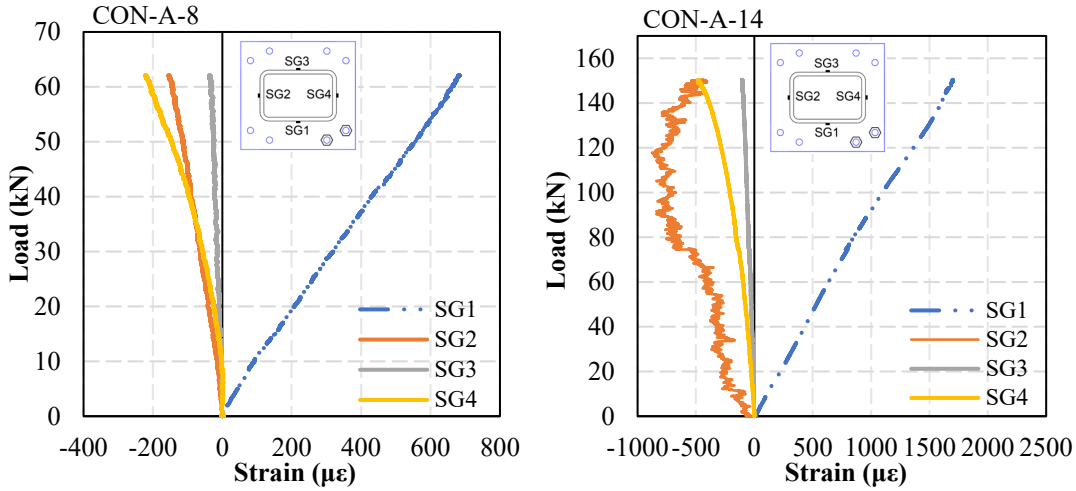

Figure 11. Strain development on column faces of Type A specimens

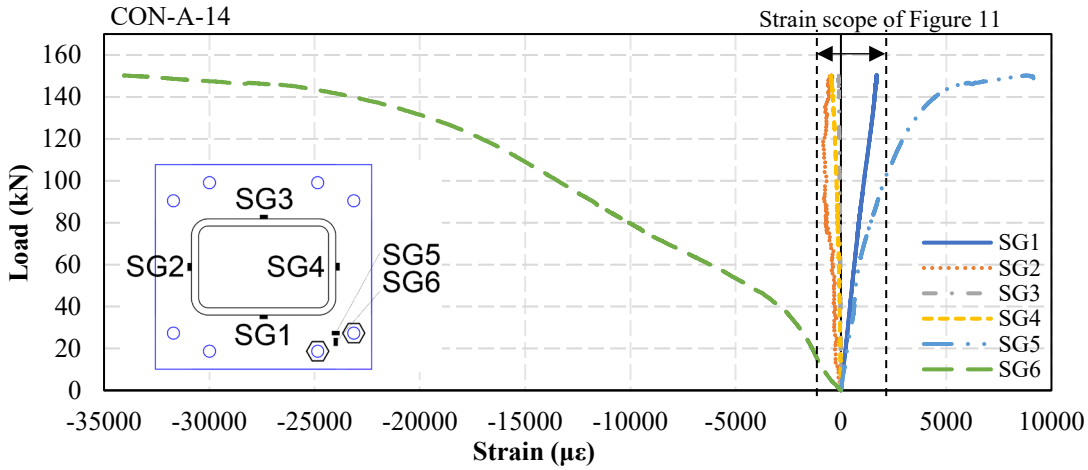

Figure 12. Strain comparison between the column and endplate of specimen CON-A-14

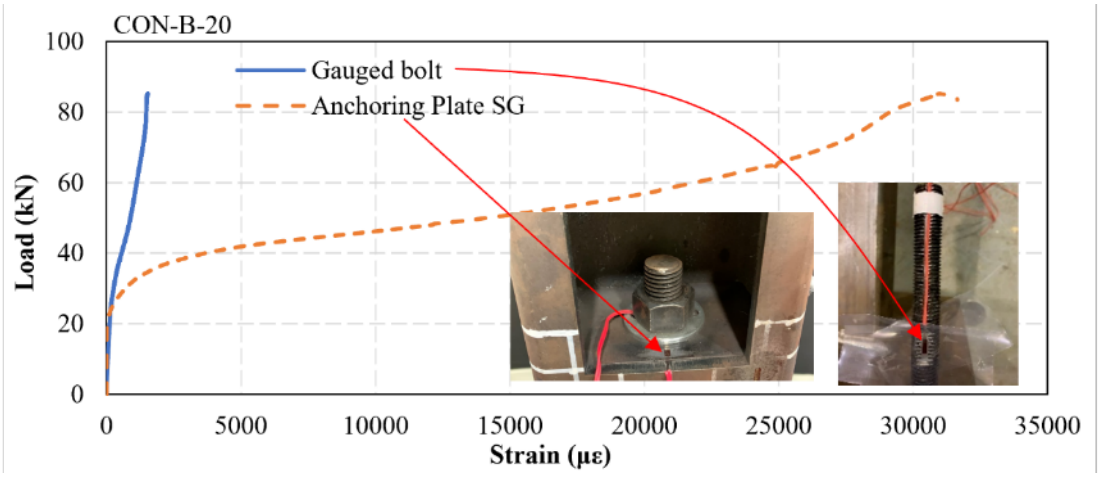

Figure 13. Strain development in the bolt and anchoring plate of specimen CON-B-20

5.4 Strain development in subassemblies of modular frames

The strain distribution and development versus the loading process at the designated positions for tested subassemblies of modular frames were summarized in Figure 14. The strains of SG1 and SG2 remained at low level for all the tested specimens, and the strain of SG3 was similar in magnitude but opposite in direction to the strain of SG4. Similar strain distribution pattern was obtained in Deng et al. (2018). This is because under the loading and boundary conditions in the test, the floor beam and ceiling beam worked almost independently. SG1 and SG2 were located in the neutral axes of the two beams, and therefore underwent low levels of strains. SG3 and SG4 were located in the upper and lower flanges of the two beams, respectively,

401 resulting in larger but opposite strains in SG3 and SG4.

402 The data from SG3, 4, 6, 8 revealed that minor yielding developed at the beam end and column
403 end before fracture occurred in the beam-to-column weld for specimens with Type B inter-
404 module connections, while no yielding developed at those positions in specimens SA-W and
405 SA-A-8. This confirmed that the fracture of the beam-to-column weld determined both the
406 strength and deformation capacities for all the five tested subassemblies of modular frames.
407 The deformation capacity and the resistance of the tested subassemblies could have been
408 improved if the premature weld fracture had been avoided. As such, it is recommended to avoid
409 the failure mode of weld fracture in modular frames.

410 For specimens with Type B inter-module connections, the strains on the two sides of the bolt
411 hole in the anchoring plate of the upper column were measured, and the results of specimen
412 SA-B-20 are presented in Figure 15. As shown, with the increase of the load, strains of large
413 magnitudes but in opposite directions developed on the two sides of the bolt hole, indicating
414 significant bearing occurred between the bolt and the anchoring plate. This revealed that the
415 bolt in the inter-module connection will be subjected to significant shear forces when modular
416 frames with Type B inter-module connections are under lateral loading. This finding is
417 noteworthy as intuitively the shear key in Type B inter-module connections is expected to
418 mainly transfer the shear force while the bolt is intended to mainly transfer the axial force.
419 Further research is needed to quantify the shear force demand on the bolt to ensure bolt safety
420 in the design of Type B inter-module connections.

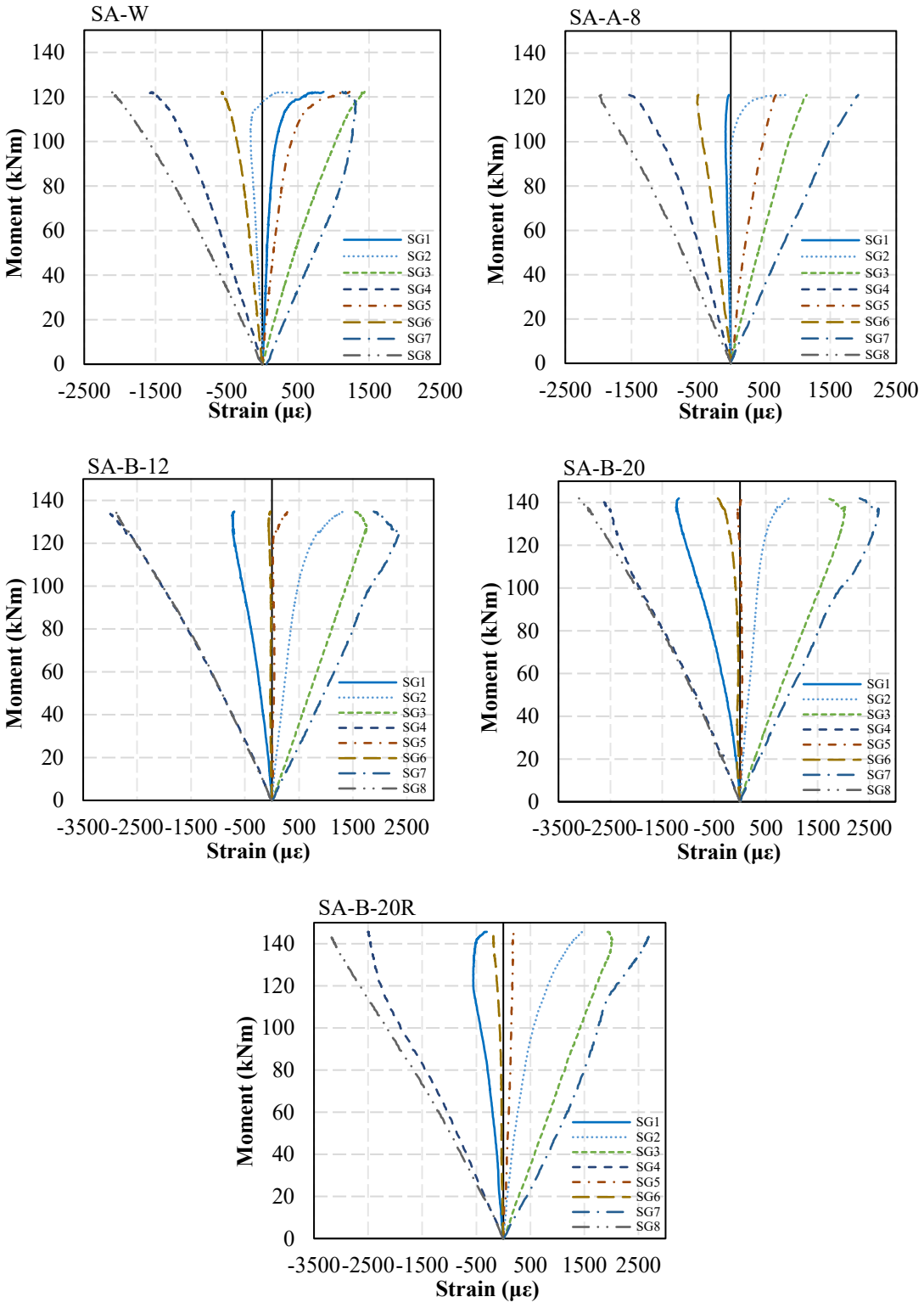

Figure 14. Strain development in the tested subassemblies of modular frames

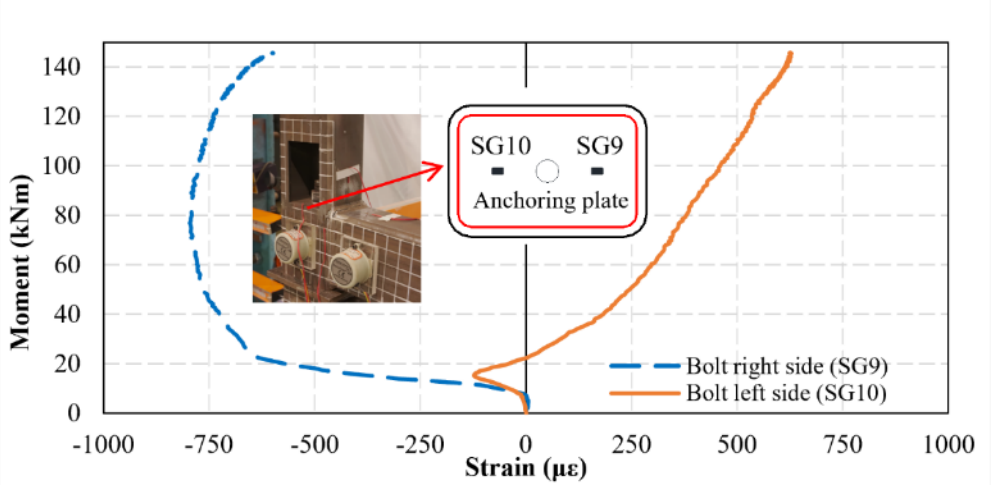

425

426 **Figure 15.** Strain development on the two sides of the bolt hole in the anchoring plate of

427 specimen SA-B-20

428 **5.5 Tensile resistance of inter-module connections**

429 Based on the failure modes observed in the tests, design formulas will be developed to estimate

430 the tensile resistance for Type A and Type B inter-module connections. The observed

431 yield/failure modes of Type A connection are bolt fracture and endplate yielding. As bolts are

432 assumed to sustain tensile forces, the resistance corresponding to bolt fracture can be calculated

433 as

$$R = nN_t^b = nA_e f_t^b \quad (1)$$

434 where A_e is the net area of a bolt, f_t^b is the ultimate strength of bolt, and n is the number of

435 bolts adopted in joint. To investigate the yielding pattern of endplates, a finite element analysis

436 was performed using ABAQUS (Dassault Systèmes, 2020). Numerical models were

437 constructed for the Type A specimens and tensile loading was applied. The models utilized 3D

438 brick elements of the type C3D8R. Nonlinear material properties, including the yield strength

439 and strain hardening, were assigned to the relevant components based on tensile coupon tests.

440 The typical yielding pattern of the endplate is illustrated in Figure 16(a). Together with the

441 experimental observation, a simplified yielding pattern was assumed for the endplate of Type

442 A connection under tensile loading, as shown in Figure 16. the corresponding yield resistance

443 can be calculated as

$$R = mL/d \quad (2)$$

444 where $m = f_y t^2/4$ and L are the unit bending resistance and the length of the assumed yield
445 line, respectively, t is the plate thickness, f_y is yield strength of steel, d is the distance from the
446 centre of the two bolt holes to the yield line.

447

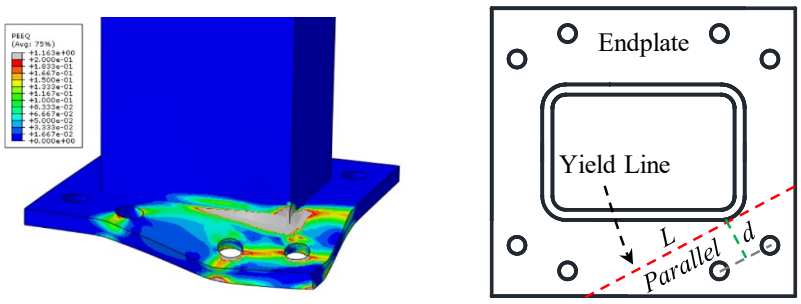

448 (a) (b)

449 **Figure 16.** Type A inter-module connections under tensile loading: (a) Typical yielding
450 development of endplate, (b) Assumed simplified yielding pattern

451 Bolt failure and anchoring plate yielding were obtained as the yield/failure modes of Type B
452 inter-module connections under tensile loading. Similarly, the resistance corresponding to bolt
453 fracture can be calculated by Eq. (1). To study the yielding pattern of the anchoring plates,
454 finite element models were also created for Type B specimens, in which elements of the type
455 C3D8R were used and the nonlinear material properties obtained through tensile coupon tests
456 were assigned. Under tensile loading, the anchoring plates in Type B inter-module connections
457 typically exhibit a yielding pattern as shown in Figure 17(a). Based on this pattern, a simplified
458 yielding pattern was assumed and is illustrated in Figure 17(b). The resistance corresponding
459 to the first yielding of the anchoring plate can be calculated as (Park and Gamble, 1999)

$$R = 4m\pi \quad (3)$$

460 where $m = f_y t^2/4$ is the unit bending resistance of the endplate, t is the plate thickness and f_y
461 is yield strength of steel.

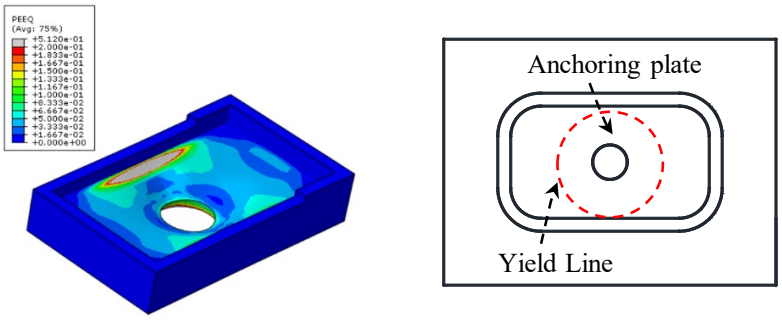

(a) (b)

Figure 17. Type B inter-module connections under tensile loading: (a) Typical yielding development of anchoring plate, (b) Assumed simplified yielding pattern

The resistances obtained from experiments and those calculated using proposed formulas are listed and compared in Table 4. For Specimens Con-A-14 and Con-B-20, strain gauge data revealed significant strains in the yield regions of the steel, as illustrated in Figures 12 and 13. As such, resistances were also calculated using the ultimate strength (f_u). The calculated resistances were found to be smaller than the corresponding resistances obtained from the tests. This discrepancy can be attributed mainly to the difference between the actual yield pattern and the simplified yield pattern assumed in the calculations. Notably, during the tests, large deformations were observed in the endplate of specimen Con-A-14 and the anchoring plate of specimen Con-B-20, which may have resulted in tensile membrane action in these plates that differs from the assumed yield pattern. It should be noted that specimens Con-B-12/12R failed due to low fabrication quality, specifically poor fitting between the bolt shank and nut, resulting in bolt thread failure. As the proposed formulas do not apply to this failure mode, the results for these two specimens are not included in the table.

Importantly, the proposed formulas in this study are based on assumed failure modes derived from experimental observations, and there are simplifications made in these assumed failure/yield modes. For instance, the exclusion of the prying action in the bolt group of Type A connections and the approximations made in the assumed yielding pattern may result in some inaccuracies. Consequently, it is vital to recognize that these formulas are intended for rough

and preliminary estimation purposes. To refine and enhance the accuracy of the formulas, a more comprehensive numerical parametric study shall be conducted.

Table 4. Resistance comparison between test results and theoretical values

Specimen	Failure mode	Resistance (kN)				
		Test	Calculated (using f_y)	Calculated (using f_u)	Calculated (f_y)/Test	Calculated (f_u)/Test
Con-A-8	Bolt failure	62.0	58.6	58.6	0.95	0.95
Con-A-14	Plate yielding	108.0	61.5	77.8	0.57	0.72
Con-B-12	Bolt thread failure	32.6	N/A	N/A	N/A	N/A
Con-B-12R	Bolt thread failure	32.1	N/A	N/A	N/A	N/A
Con-B-20	Plate yielding	59.5	27.7	35.7	0.47	0.60

5.6 Simplified beam-to-column model

To facilitate the understanding of the behavior of modular frames under lateral loading, a simplified beam-to-column model similar to the model for conventional frames was proposed and shown in Figure 18. Firstly, the second moment of area of the equivalent beam in the simplified model, $I_{b,eqv}$, was determined based on the experimental test results. Secondly, the moment-rotation behavior of the equivalent beam-to-column joint is classified based on the criteria in EN-1993-1-8 (CEN, 2005).

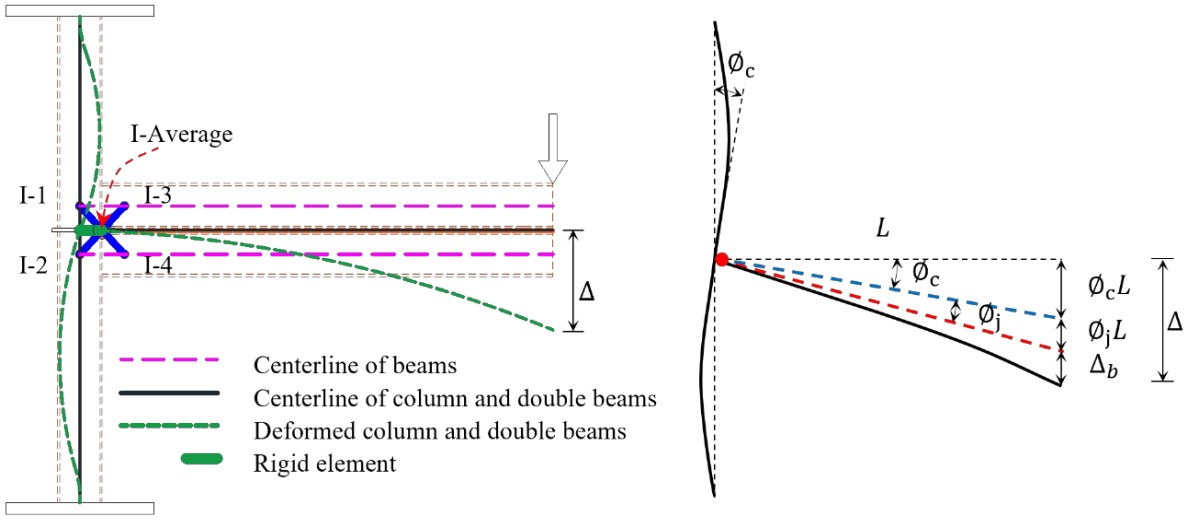

(a) Conceptual deformation shape of subassembly of modular frame

(b) Simplified beam-to-column model

Figure 18. Simplified beam-to-column model

Figure 18(b) shows the kinematic relationship of the deformed beam-column subassembly under vertical loading at beam end, in which $\emptyset_c$ = rotation of the column, $\emptyset_j$ = rotation of the beam-column joint, Δ = vertical displacement of the beam at the position of loading, Δ_b = vertical displacement of the beam caused by flexural deformation of the beam itself, L = length of the beam from the loading point to the column face. By the average rotation derived from the four inclinometers (I-1 to I-4) installed on the tested specimens as shown in Figure 6, $\emptyset_j + \emptyset_c$ can be obtained. Subsequently, Δ_b can be estimated as

$$\Delta_b = \Delta - (\emptyset_j + \emptyset_c) \cdot L \quad (4)$$

Finally, as the beams in the tested specimens remained essentially elastic, the second moment of area of the equivalent beam in the simplified model can be obtained as

$$I_{b,eqv} = FL^3 / 3E\Delta_b \quad (5)$$

Table 5 lists the values of $I_{b,eqv}$ for the tested five specimens. For the purpose of comparison, the summation of the second moment of area of the floor beam and the ceiling beam was also calculated, i.e.,

$$I_{b,sum} = I_{floor} + I_{ceiling} \quad (6)$$

As shown in Table 5, the values of $I_{b,eqv}/I_{b,sum}$ range from 1.32 to 1.59. For design of conventional moment frames under seismic loading, the "strong column-weak beam" principle is usually applied as this reduces the likelihood of the formation of story mechanisms (Chopra, 2012). The obtained values of $I_{b,eqv}/I_{b,sum}$ revealed that, in order to implement the "strong column-weak beam" principle for modular frames, in addition to $I_{b,sum}$ of the floor beam and the ceiling beam, extra second moment of area (32% to 59% of $I_{b,sum}$ were obtained for the tested specimens) shall be considered in the calculation of beam strength. More research is needed to further quantify the flexural strength of the floor and ceiling beams combined under lateral loading.

Table 5. Comparison between $I_{b,eqv}$ and $I_{b,sum}$

Specimen	SA-W	SA-A-8	SA-B-12	SA-B-20	SA-B-20R
$I_{b,test}$ $(\times 10^6\ mm^4)$	11.76	12.68	10.92	10.57	10.53
$I_{b,sum}$ $(\times 10^6\ mm^4)$	7.98	7.98	7.98	7.98	7.98
$I_{b,eqv}/I_{b,sum}$	1.47	1.59	1.37	1.33	1.32

518

519 According to the definition of the beam-to-column joint location in structure from EN-1993-1-
520 8 (CEN, 2005), the moment applied to the beam-to-column joint should be calculated as $M = FL$ with F = the vertical force applied on the loading point on beam and L = the distance from
521
522 loading point to the column face. Figure 19 shows the moment-rotation (i.e., M-$\emptyset_j$) curves of
523 the tested five specimens (Fang et al., 2018). Based on EN-1993-1-8 (CEN, 2005), the joint
524 may be classified as rigid, nominally pinned or semi-rigid by comparing its initial rotational
525 stiffness with the classification boundaries related to the rigidity of the adjacent beams EI_b/L_b,
526 as detailed in Table 6. As can be seen, the equivalent beam-to-column joints in specimens with
527 either Type A or Type B inter-module connections qualified as semi-rigid, while that of the
528 specimen with welded inter-module connections qualified as rigid. This is because both Type
529 A and Type B inter-module connections allow a certain degree of rotation, although all the
530 beams and columns are almost rigidly connected through welds. Being classified as semi-rigid
531 indicates that the modular frame with the proposed Type A or Type B inter-module connections
532 will have smaller global lateral stiffness as compared with conventional moment frames with
533 rigid beam-to-column connections. The rotational flexibility offered by semi-rigid connections
534 can help in accommodating small rotations induced by lateral loads, redistributing forces,
535 which shall be taken into account in the global structural analysis of modular frames.

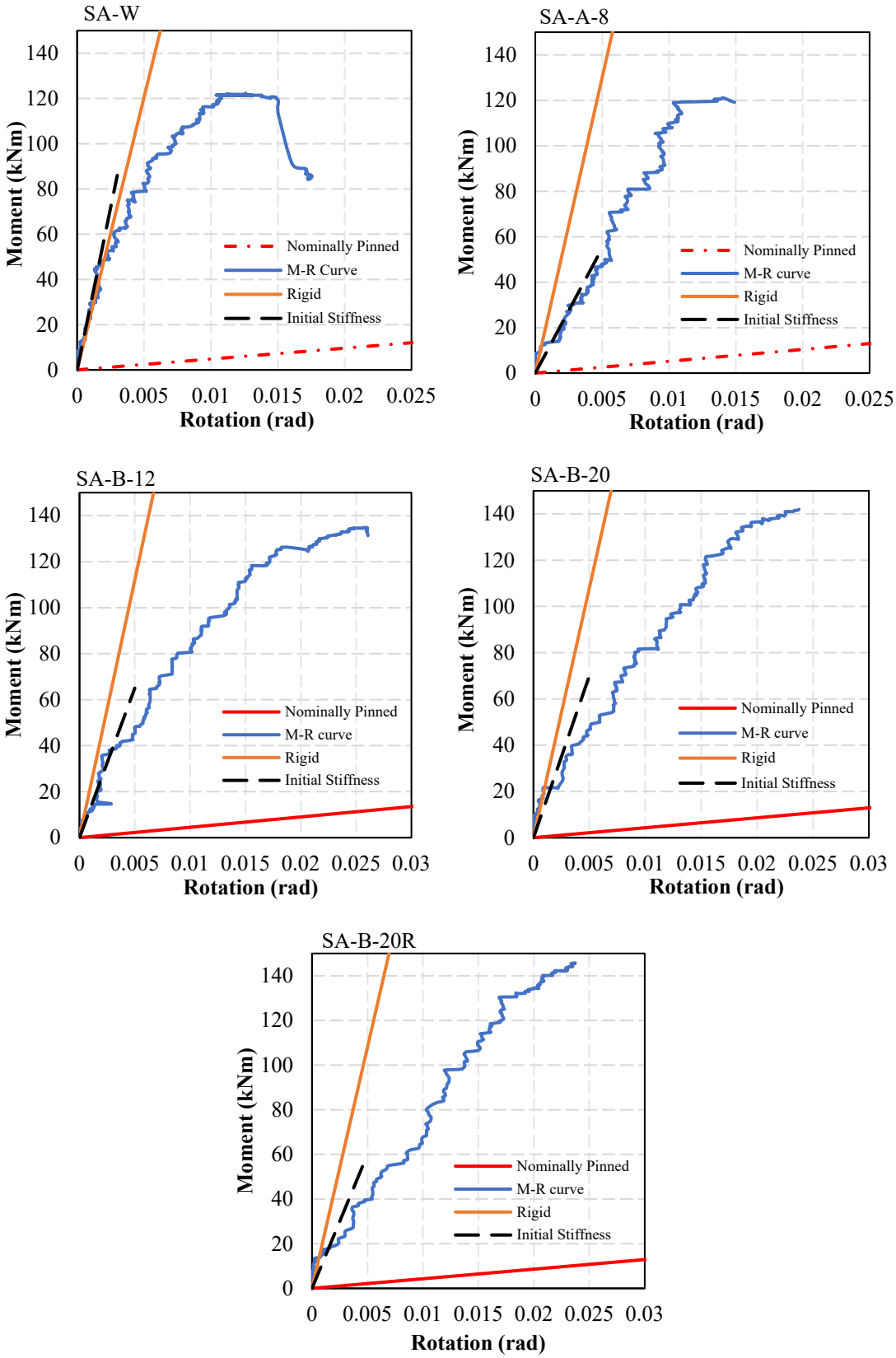

Figure 19. Moment-rotation (M-R) curves of tested subassemblies of modular frames

Table 6. Stiffness classification of beam-to-column connections.

Specimen	Stiffness $S_{j,i}$ (kNm/rad)	EI_b/L_b	$S_{j,i}/(EI_b/L_b)$	Classification (for moment resisting frames)
SA-W	28,700	963.1	29.8	Rigid
SA-A-8	11,000	1038.6	10.6	Semi-rigid
SA-B-12	13,000	894.7	14.5	Semi-rigid
SA-B -20	14,000	865.6	16.2	Semi-rigid
SA-B -20R	12,000	862.2	13.9	Semi-rigid

Note:
(1) L_b = span of the beam (center-to-center of columns).
(2) For moment resisting frames: Rigid: $S_{j,i}/(EI_b/L_b)\geq 25$; Semi-rigid: $0.5 < S_{j,i}/(EI_b/L_b) < 25$; Nominal-pinned: $S_{j,i}/(EI_b/L_b) \leq 0.5$.

6 Conclusions

This study investigates two types of bolted inter-module connections for modular structures that are simple and quick to assemble, require minimal operational space, and have the self-aligning feature. These two types are referred to as Type A and Type B inter-module connections, and the components and construction steps are elaborated for each of them. To investigate the tensile behavior of the proposed inter-module connections, five pull-out tests were conducted. Additionally, five subassemblies of modular frames with the proposed inter-module connections were tested to examine their global behavior under lateral loading. The key findings of this study are concluded as follows:

1. The yield/failure modes of Type A inter-module connections under tensile loading include bolt fracture and yielding of endplate in the form of bending along the bolt line. Yielding of the endplate prior to bolt fracture is recommended as this can lead to a more ductile response.
2. For Type B inter-module connections under tensile loading, the yield/failure modes include bolt fracture and yield of the anchoring plate. The anchoring plate initially resists the axial load through out-of-plane deformation. After large deformation, the membrane mechanism will form in the anchoring plate, which results in a further

563 increase in the resistance and a partial restoration of the stiffness. Bolt fracture is
564 recommended to be prevented in order to achieve ductile behavior in Type B inter-
565 module connections.
566 3. Fracture of beam-to-column weld was identified to be the main failure mode for all of
567 the test subassemblies of modular frames, which revealed that modular frames with
568 welded beams to columns are prone to premature fracture of beam-to-column welds.
569 As the premature failure in beam-to-column welds usually results in abrupt loss of
570 resistance and prevents the further development of both ductility and resistance, such
571 failure mode is recommended to be avoided in design of modular frames.
572 4. Modular frames with Type B inter-module connections showed larger deformation
573 capacities under lateral loading than those with Type A or welded inter-module
574 connections. It is believed to be attributed to the fewer welds used in Type B inter-
575 module connections, which resulted in less severe heat-affected zones and fewer
576 welding defects.
577 5. When modular frames with Type A inter-module connections are subjected to lateral
578 loading, bending of endplate around the bolts will occur which will result in the
579 separation of the two columns and flexural discontinuity in the inter-module connection.
580 6. For modular frames with Type B inter-module connections, relative sliding of the two
581 columns will occur in the inter-module connection until the shear key contacts the
582 columns when the frame is subjected to lateral loading. Although the shear key is
583 assumed to mainly resist the shear force in Type B inter-module connections,
584 significant shear force was found in the bolt, which shall be considered in the design of
585 the bolt in Type B inter-module connections.
586 The experimental tests also set the benchmark for further numerical studies at both the
587 connection level and the system level for modular frames. However, in order to draw

588 conclusive findings regarding the impact of various parameters on the strength and ductility,
589 as well as to provide substantial design guidance, further numerical parametric studies are
590 required. Moreover, as the connections were not loaded in a cyclic manner, the cyclic behavior
591 and the damping capacity of the connections could not be characterized. As many lateral loads,
592 such as earthquake excitation, are cyclic in nature, it is essential to investigate the cyclic
593 behavior and damping capacity of the connections in further studies.

594 **Acknowledgments**

595 The authors sincerely acknowledge the support received from the Innovation and Technology
596 Fund - Nano and Advanced Materials Institute (ITF-NAMI) for the project "Hong Kong
597 Modular Integrated Construction (MiC) Innovations" (Grant number: PolyU/ZS12) and from
598 the Chinese National Engineering Research Centre for Steel Construction (Hong Kong Branch)
599 at The Hong Kong Polytechnic University. The loading of the specimens was conducted at the
600 Structural Engineering Research Laboratory at The Hong Kong Polytechnic University
601 (https://www.polyu.edu.hk/cee/about-cee/facilities/). The authors would like to thank Mr. Chi-
602 Fai Cheung, Mr. Qi Ma, and Mr. Hai-Xin Liu for their assistance during the experiments.

603 **References**

604 Chen, Z., Liu, J., Yu, Y., Zhou, C. and Yan, R. (2017a). Experimental study of an innovative
605 modular steel building connection. *Journal of Constructional Steel Research*, *139*, pp.69-
606 82.
607 Chen, Z., Li, H., Chen, A., Yu, Y. and Wang, H. (2017b). Research on pretensioned modular
608 frame test and simulations. *Engineering Structures*, *151*, pp.774-787.
609 Cho, B.H., Lee, J.S., Kim, H. and Kim, D.J. (2019). Structural performance of a new blind-
610 bolted frame modular beam-column connection under lateral loading. *Applied*
611 *Sciences*, *9*(9), p.1929.
612 Chopra A. K. (2012). Dynamics of structures: theory and applications to earthquake
613 engineering. 4th ed. USA: *Pearson Prentice Hall*.
614 Dassault Systèmes. (2020). ABAQUS (Version 2020) [Computer software]. Velizy-
615 Villacoublay, France: Dassault Systèmes.

Deng, E.F., Zong, L., Ding, Y., Dai, X.M., Lou, N. and Chen, Y. (2018). Monotonic and cyclic response of bolted connections with welded cover plate for modular steel construction. *Engineering Structures*, *167*, pp.407-419.

EN ISO 6892-1:2019. (2019). Metallic materials—Tensile testing Part 1: Method of test at room temperature (ISO 6892-1:2019), Brussels, Belgium.

C.E.N. (2005). Eurocode 3: Design of steel structures, Part 1-8: Design of joints. Brussels: EN1993-1-8, European Committee for Standardization.

Fang, C., Yam, M.C., Chan, T.M., Wang, W., Yang, X. and Lin, X. (2018). A study of hybrid self-centring connections equipped with shape memory alloy washers and bolts. *Engineering Structures*, 164, pp.155-168.

Ferdous, W., Bai, Y., Ngo, T. D., Manalo, A., & Mendis, P. (2019). New advancements, challenges and opportunities of multi-storey modular buildings–A state-of-the-art review. *Engineering Structures*, 183, 883-893.

He, X.H.C., Chan, T. M. (2023). Classification system for inter-and intra-module joints in non-sway steel MiC structures. *Journal of Constructional Steel Research*, 206, 107913.

He, X.H.C., Chan, T.M. and Chung, K.F. (2021). Effect of inter-module connections on progressive collapse behaviour of MiC structures. *Journal of Constructional Steel Research*, *185*, p.106823.

Hu, Y.F., Jiang, H., Chan, T.M., Wu, Y.M., Zhang, J., Liu, Y.F. and Zhu, H.G. (2021). A detachable modular integrated constructions module. Patent No. HK30037714, Short-term Patent, Patents Registry, Intellectual Property Department, The Government of Hong Kong Special Administrative Region.

Hu, Y.F., Jiang, H., Chan, T.M., Wu, Y.M., Zhang, J., Liu, Y.F. and Zhu, H.G. (2022). A detachable modular integrated constructions module. Patent No. CN 215406584 U, Utility Model Patent, China National Intellectual Property Administration, The Government of People's Republic of China.

Kamali, M., & Hewage, K. (2016). Life cycle performance of modular buildings: A critical review. *Renewable and sustainable energy reviews*, 62, 1171-1183.

Khan, K. and Yan, J.B. (2020). Finite element analysis on seismic behaviour of novel joint in prefabricated modular steel building. *International Journal of Steel Structures*, *20*(3), pp.752-765.

Lacey, A.W., Chen, W., Hao, H. and Bi, K. (2019b). Review of bolted inter-module connections in modular steel buildings. *Journal of Building Engineering*, *23*, pp.207-219.

Lacey, A.W., Chen, W., Hao, H., Bi, K. and Tallowin, F.J. (2019a). Shear behaviour of post-

650 tensioned inter-module connection for modular steel buildings. *Journal of Constructional*
651 *Steel Research*, *162*, p.105707.
652 Lawson, R. M., Ogden, R. G., & Bergin, R. (2012). Application of modular construction in
653 high-rise buildings. *Journal of architectural engineering*, 18(2), 148-154.
654 Lawson, R. Ogden, C. Goodier. (2014). Design in modular construction. *CRC Press*.
655 Lyu, Y. F., Li, G. Q., Cao, K., Zhai, S. Y., Li, H., Chen, C., & Wang, Y. Z. (2021). Behavior
656 of splice connection during transfer of vertical load in full-scale corner-supported modular
657 building. Engineering Structures, 230, 111698.
658 Nadeem, G., Safiee, N.A., Bakar, N.A., Abd Karim, I. and Nasir, N.A.M. (2021). Connection
659 design in modular steel construction: A review. In *Structures* (Vol. 33, pp. 3239-3256).
660 Navaratnam, S., Ngo, T., Gunawardena, T. and Henderson, D. (2019). Performance review of
661 prefabricated building systems and future research in Australia. *Buildings*, 9(2), p.38.
662 Park, K. S., Moon, J., Lee, S. S., Bae, K. W., & Roeder, C. W. (2016). Embedded steel column-
663 to-foundation connection for a modular structural system. Engineering Structures, 110, 244-
664 257.
665 Park, R. and Gamble, W.L. (1999). Reinforced concrete slabs. *John Wiley & Sons*.
666 Sanches, R., Mercan, O. and Roberts, B. (2018). Experimental investigations of vertical post-
667 tensioned connection for modular steel structures. *Engineering Structures*, *175*, pp.776-789.
668 Shan, S., Looi, D., Cai, Y., Ma, P., Chen, M.T., Su, R., Young, B. and Pan, W. (2019).
669 Engineering modular integrated construction for high-rise building: a case study in Hong
670 Kong. In *Proceedings of the Institution of Civil Engineers-Civil Engineering* (Vol. 172, No.
671 6, pp. 51-57). Thomas Telford Ltd.
672 Wang, C., & Chan, T. M. (2023). Seismic design and parametric study of steel modular frames
673 with distributed seismic resistance. *Thin-Walled Structures*, 182, 110325.
674